Stony Brook University

Self-supported PANI /WO_3 Hybrid Photocatalyst for Dye Remediation

A Thesis Presented

by

Xicheng Jia

to

The Graduate School

in Partial Fulfillment of the Requirements

for the Degree of

Master of Science

in

Materials Science and Engineering

Stony Brook University

May 2015

Stony Brook University

The Graduate School

Xicheng Jia

We, the thesis committee for the above candidate for the

Master of Science Degree, herehy recommend

acceptance of this thesis.

Perena Gouma
Professor Department of Materials Science and Engineering

Jonathan. C. Sokolov
Professor Department of Materials Science and Engineering

Taejin Kim
Assistant Professor Department of Materials Science and Engineering

This thesis is accepted by the Graduate School

Charles Taber
Interim Dean of the Graduate School

Abstract of the Thesis

Self-supported PANI /WO_3 Hybrid Photocatalyst for Dye Remediation

by

Xicheng Jia

Master of Science

in

Materials Science and Engineering

Stony Brook University

2015

Polyaniline (PANI), one of the most important conducting polymers, has been studied intensely in recent years for its unique properties. Tungsten trioxide (WO_3), on the other hand, is an important functional semiconductor. In this work, a hybrid mat based on PANI and WO_3 was synthesized via spin coating and tested as a visible light photocatalyst. A PANI/TiO_2 composite photocatalyst was made in the same way and its photocatalytic response was compared to that of PANI/WO_3 and of pure WO_3, respectively, under visible light for the remediation of methylene blue in water. Furthermore, the effect of salinity on the spontaneous photolysis of Methylene blue in the absence of a catalyst has been studied.

From the spectroscopic study results of WO_3/PANI mat, TiO_2/PANI mat and pure WO_3, the hybrid WO_3/PANI mat shows a very good degradation rate of Methylene blue solution, which is almost 88%, compare to around 39% degradation rate of TiO_2/PANI and 62% of pure WO_3 (same weight of the WO_3 percent in WO_3/PANI), the result show a very effective improvement of photocatalytic activity of WO_3 by modification with PANI. Besides, the

spectroscopic results of spontaneous photolysis of methylene blue also show that the salinity of the content of NaCl has a slightly inhibiting influence on methylene blue degradation.

Dedication Page

Dedicated to my dear Parents.

Table of Contents

1.1 Photocatalysis 3

1.2 Factors Influencing Photocatalytic Efficiency 7

1.2.1 Nature of the photocatalyst 7

1.2.2 Quantity of the photocatalyst 7

1.2.3 Concentration of the substrate 8

1.2.4 Intensity of light 8

1.2.5 pH level 8

1.2.6 Temperature 8

1.3 Introduction to Tungsten Oxide (WO_3) 9

1.3.1 Structure of WO_3 9

1.4 Introduction to Polyaniline (PANI) 11

1.4.1 Structure of PANI 12

1.4.2 Doping mechanism of PANI 13

1.4.3 Solubility of PANI in some common organic solvents 14

1.5 Potential advantages of WO_3/PANI composite film 15

1.6 The matrix of Cellulose Acetate 16

1.7 Spin coating 17

1.7.1 Parameters that affect spin coating 18

1.8 Methylene Blue 19

1.9 Salinity and sodium chloride 20

Chapter 2: Materials Used 23

Chapter 3: Methods of Preparation 24

3.1 Preparation of WO_3/PANI hybrid photocatalyst 24

3.1.1 Preparation of PANI (H^+) 24

3.1.2 Preparation of PANI(H+) and WO_3 solution 24

3.1.3 Spin coating to get the WO_3/PANI thin film 25

3.1.4 Film isolating from the glass matrix 25

3.1.5 Preparation of TiO_2/PANI thin film 26

3.1.6 Preparation of different salinity NaCl solution 26

Chapter 4: Characterization techniques 28

4.1 Scanning Electron Microscopy (SEM) 28

4.2 Energy Dispersive X-Ray Spectroscopy (EDS) 28

4.3 Thermogravimetric Analysis (TGA) 29

Photocatalytic Test 30

4.4 Ultraviolet-visible Spectroscopy (UV-vis) 31

Chapter 5: Result and Discussions 33

5.1 Characterization with SEM with EDS 33

5.2 Characterization using Thermogravimetric Analysis (TGA) 35

5.3 UV-vis Spectroscopic Analysis 36

5.3.1 Absorbance graphs for visible light degradation 37

5.3.2 Comparative analysis of degradation under UV light 41

5.4 Methylene Blue Solution Photolytic Analysis 42

5.4.1 Absorbance Graphs for photolytic degradation 43

5.4.2 Comparative analysis of photolytic degradation under UV light 47

Chapter 6: Conclusions 49

Future work 50

Reference 51

List of figures

Figure 1: Diagram of some semiconductors' valence and conduction band energy [21] 3
Figure 2: Schematic of the process in a semiconductor photocatalyst that is excited by a photon: (p) photogeneration of electron/hole pair, (q) surface recombination, (r) recombination in the bulk, (s) diffusion of acceptor and reduction on the surface of semiconductor, and (t) oxidation of donor on the surface of semiconductor particle. [27] 6
Figure 3: Crystal structure of tungsten (VI) oxide [52] 10
Figure 4: Structure of PANI with two units [66] 12
Figure 6: PANI emeraldine base doping with HCl [69] 14
Figure 7: Molecular structure of Cellulose Acetate [66] 16
Figure 8: The brief procedures of spin coating [81] 17
Figure 9: Some factors that affect spin coating materials (Source: Brewer Science Inc) 18
Figure 10: Methylene blue crystal structure [84] 19
Figure 11: The sodium chloride crystal structure (Source: Washington University in St. Louis, 2005) 21
Figure 12: WO_3/PANI thin film 25
Figure 13: TiO_2/PANI thin film 26
Figure 14: UV-vis spectrometer set-up (Source: 2001 B.M Tissue) 31
Figure 15: SEM images of (a)upper layer at Mag=300x; (b)upper layer at Mag=1.00kx; (c) bottom layer at Mag=300x; (d)bottom layer at Mag=1.00kx 34
Figure 16: EDS of the WO_3/PANI film 35
Figure 17: TGA analysis of WO_3/PANI film 36
Figure 18: Graph of absorbance intensity versus wavelength for WO_3/PANI film under visible light 38
Figure 19: Graph of absorbance intensity versus wavelength for TiO_2/PANI film under visible light 39
Figure 20: Graph of absorbance intensity versus wavelength for WO_3 under visible light 40
Figure 21: Graph of the degradation of the three photocatalysts under visible light 41
Figure 23: Graph of absorbance versus wavelength for 0g NaCl methylene blue solution 43

Figure 24: Graph of absorbance versus wavelength for 0.5g NaCl methylene blue solution 44
Figure 25: Graph of absorbance versus wavelength for 1.0g NaCl methylene blue solution 45
Figure 26: Graph of absorbance versus wavelength for 1.5g NaCl methylene blue solution 46
Figure 27: Graph of the degradation of four different salinity solutions under visible light 48

List of Tables

Table 1: Band gap energies of semiconductors 4
Table 2: Different phases of WO3 under different temperature [50] 10
Table 3: The solubility of PANI in different solvents [74] 14
Table 4: The salinity value of different waters 21
Table 5: The properties of chemicals used to synthesize the photocatalystic film 23
Table 6: Degradation percentage of catalyst under visible light at 180 minutes 40
Table 7: Degradation percentages of different salinity solutions under visible light at 180 minutes 47

Acknowledgements

I am very grateful to my Professor Perena Gouma for giving me this great opportunity to participate in this project. She was always there encouraging me and giving me a lot of great advice when I met difficulties during my research work. I feel so lucky to have such a great supervisor who is always with a big smile when every little improvement I made in my work. The project was partially supported by the NSF grant: DMR-1106168.

I also want to thank Professor Sokolov and Professor Kim for serving as my committee members and all the help they gave.

I would like to thank Dr. Jim Quinn for helping me do the SEM test, thank Xiaojun Chan for helping me do the TGA test and thank Selda Tocpu for teaching me use the lab facilities.

I would like to extend my thanks to all my labmates: Jiahao Huang, Gagan Jodhani, Chao Han and Yan Li for their help and the friendly lab environment they make.

A special thank you to my parents who always support and encourage me, and all the love they give me, I love them very much.

Chapter 1: Introduction

Photocatalysis is enabled by nano semiconductor materials [1]. By exposing to light irradiation, nano semiconductor materials can transfer solar energy into chemical energy, by which photocatalysts can accelerate either synthesis or degradation of compounds (organics or inorganics), this process is called photocatalysis [2]. In 1972, Fujishima and Honda first reported that Titanium dioxide could be used as photocatalyst to produce Hydrogen via water splitting [3]. During that period the world was experiencing energy crisis, it has great practical significance using solar energy to prepare hydrogen in order to relieve the energy shortage, under that circumstance this new idea immediately aroused enormous attention. By the year 1977, Bard used TiO_2 as the catalyst to oxidate CN^- into OCN^-, which opened a new way for water pollutant treatment [4]. In fact, in the middle of 20th century, the period around 1950s to 1960s, there were some studies on the photocatalysis efficiency of ZnO, mainly based on some photo-oxidation reactions, such as: preparing ozone from oxygen, hydrogen peroxide from oxygen and water [5]. Since the quantum yield (per absorbed photon can give rise to the times of the chemical reaction) was very low, there was no practical application for the chemical synthesis, leading to barely focus in this field. Modify the particle's size to nanosized scale is a efficient way to improve quantum yield due to the chemical activities can be greatly improve, the advantages of accepting nanosized level semiconductors are listed as flowing: firstly, high ratio of surface area to volume; secondly, greatly improve the absorption cross section; thirdly, accelerate the carrier diffusion on the interface in order to reduce recombination [6]. There has been reported that the conversion of toluene photo-oxidation is greatly increased by using a much smaller size TiO_2 particle [7].

In the 1990s, thanks to the rapid development of nanotechnology, an excellent opportunity arose for the application of photocatalytic technology. Meanwhile, due to the development of global industrialization, environmental pollution is worsening, environmental protection conservation and sustainable development became an issue that must be considered, so the development of photocatalytic materials became more and more important [8-12].

In recent years, semiconductor photocatalyst has been a promising research topic due to it has shown great potential in treating environmental pollution. Many semiconductor materials have been applied in the photocatalytic oxidation of organic compounds, such as TiO_2, SnO_2, Fe_2O_3, ZnO, etc [13]. Among all of these promising semiconductor materials, WO_3 is attracting a lot of foci and more and more researchers start to discover WO_3 as an effective photocatalyst under visible light.

Meanwhile, Polyaniline(PANI) as one the most important conducting polymers involves many advantages, such as versatile redox behavior, excellent chemical stability, electrochromic properties and so more [14-16]. It has been reported that the combination of semiconductor materials like ZnO and CdS, with PANI show very good photocatalytic activities [17-18]. Besides, PANI and WO_3 are both electron and proton conductors, it seems a promising combination of WO_3 and PANI composite materials.

1.1 Photocatalysis

Photocatalysis can be simply defined as the acceleration of a photoreaction by the presence of a catalyst [2]. Photocatalytic reactions can happen when the energy of an absorbed photon is greater that or at least equal to the band gap energy of that targeted semiconductor [11]. Band gap energy can be described as the energy difference between the conduction band and valence band in semiconductors [19]. Band positions and redox potentials of the semiconductor play a very important role on photoinduced electrons transferring because the electrons transferring occur in the absorbed species on the semiconductor photocatalyst [20].

Figure 1 shows some semiconductors' valence and conduction band energy.

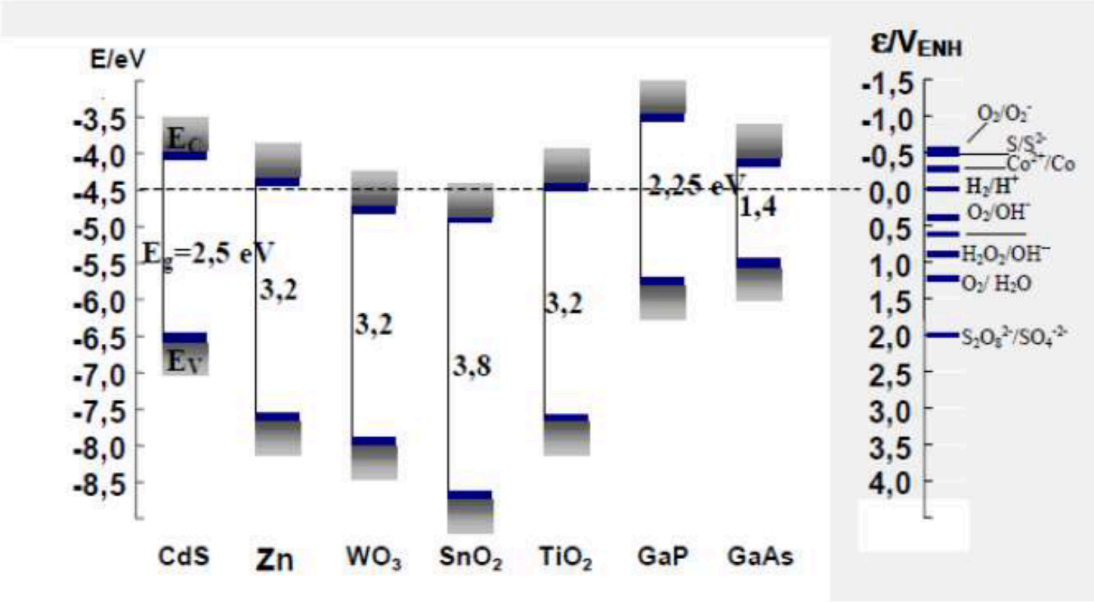

Figure 1: Diagram of some semiconductors' valence and conduction band energy [21]

The table 1 below shows some semiconductors' band gap energy in decreasing order of energy:

Table 1: Band gap energies of semiconductors

photocatalyst	Band-gap energy (eV)
Si	1.1
WSe_2	1.2
CdS	2.4
WO_3	2.4-2.8
V_2O_5	2.7
SiC	3.0
TiO_2 Rutile	3.02
Fe_2O_3	3.1
TiO_2 anatase	3.2
ZnO	3.2
$SrTiO_3$	3.2
SnO_2	3.5
ZnS	3.6

A photocatalytic reaction will be initiated when a photon hit an excited atom, leads to the electrons (e^-) of the excited atom fly away from their full valence band, and holes (h^+) coming up, then these electrons jump to the empty conduction band [22-25]. When the photoexcited electrons reach the conduction band, they come as absorbed photon energy ($h\upsilon$) that is equal to or greater than the band gap of the semiconductor photocatalyst. The electron hole pairs (e^- - h^+) will be generated in the end. Then following are some chain reactions being widely used [21]:

Photoexcitation: $TiO_2 + h\upsilon \rightarrow e^- + h^+$ (1)

Oxygen ionosorption: $(O_2)\ ads + e^- \rightarrow O_2\bullet^-$ (2)

Ionization of water: $H_2O \rightarrow OH^- + H^+$ (3)

Protonation of superoxides: $O_2\bullet^- + H^+ \rightarrow HOO\bullet$ (4)

From the equation (4) showed above, we could see that O_2 can scavenge H+ to produce hydroperoxyl radicals, and the formed hydroperoxyl radicals also can react with e^- and H^+, through that process doubles the photohole lifetime:

$$HOO\bullet + e^- \rightarrow HO_2^- \quad (5)$$

$$HOO^- + H^+ \rightarrow H_2O_2 \quad (6)$$

Besides, photon energy (E) and the threshold wavelength (λ_g), which is the greatest wavelength of radiation required for the emission of electrons, have such relationship that can be described by Planck's relation:

$$E = h\upsilon \quad (7)$$

$$\upsilon = c/\lambda_g \quad (8)$$

Where h is the Planck constant, υ is the frequency and c is the speed of light. Thus the threshold wavelength (λ_g) can also be described as

$$\lambda_g = hc/E_g \quad (9)$$

As an example, the TiO_2 (anatase) has the band gap energy E_g=3.2ev as showed in table 1, so according the chain equations above, we can get its absorption threshold is 380 nm [26].

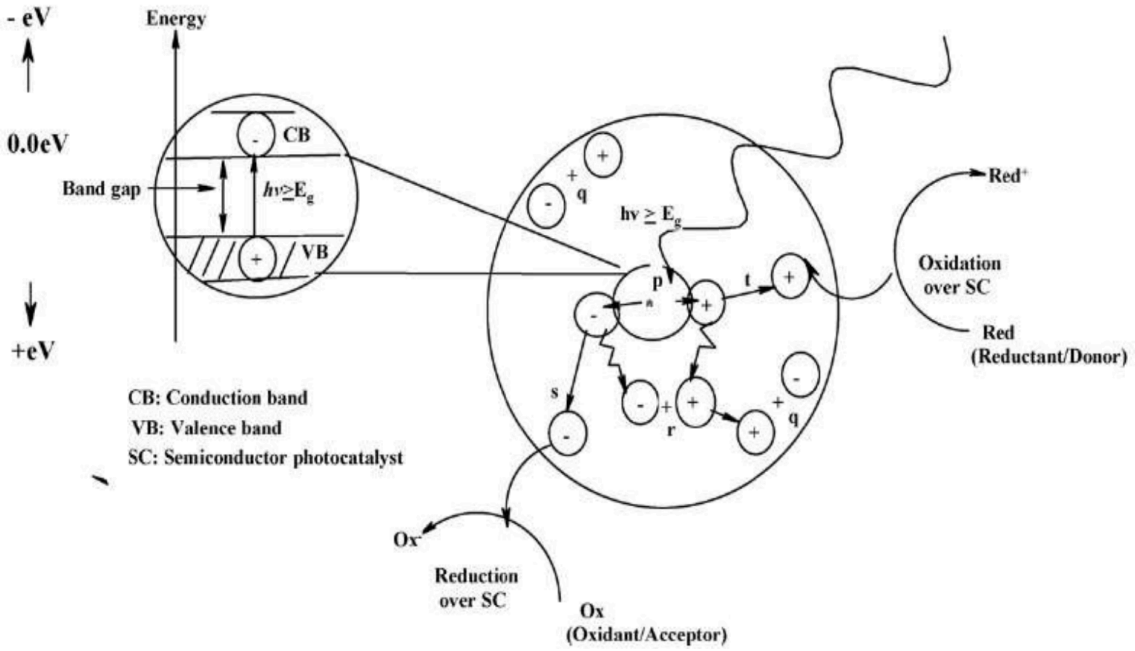

Figure 2: Schematic of the process in a semiconductor photocatalyst that is excited by a photon: (p) photogeneration of electron/hole pair, (q) surface recombination, (r) recombination in the bulk, (s) diffusion of acceptor and reduction on the surface of semiconductor, and (t) oxidation of donor on the surface of semiconductor particle. [27]

As shown in figure 2, in the photocatalytic process, once the charge separation occurs, there are several ways for the photogenerated electrons and holes to go. Electrons from organic contaminate can be given away to the holes that at the surface of the photocatalyst, which also can steal away electrons that from hydroxyl nucleophiles and then create hydroxyl, the organics will be subsequently broken down by these hydroxyl radicals, this process is called AOP (Advanced Oxidation Process) [28]. AOPs are very important reactions cause photocatalysis can be expressed as a combination of photochemistry and catalysis. The most efficiency photocatalytic degradation can be described as all the contaminants are completely degraded, which means decomposition of organics to carbon dioxide, water, mineral acid and inorganic ions [29]. There are many practical applications based on photocatalysis to treat contaminants. For example, photocatalysis is used in cleaning contaminated Nitrogen Oxides from air streams

[30], treating wastewater that is polluted by organics and metals [31], oxidizing amino acids in river [32] and so forth.

1.2 Factors Influencing Photocatalytic Efficiency

Many factors may affect the efficiency of photocatalyst, the following are some main ones:

1.2.1 Nature of the photocatalyst

It has been known that the quantities of the photons that strike the photocatalyst have an influence on the reaction rate [33]. That means the reactions can happen only on the absorbed sites at the surface of semiconductor photocatalyst. The morphology of the photocatalyst surface depends on particle shape, size, and agglomeration during photocatalytic oxidation [34]. In order to satisfy the requirements for practical application, many processing techniques for photocatalysts have been updated, modified, tested, and developed [35-36]. For instance, it has been reported that TiO_2 has higher activities at a nanometer scale [37]. It has also been reported that the nanosized TiO_2/ZnO composite greatly improve the degradation rate of methylene blue solution [38].

1.2.2 Quantity of the photocatalyst

A change in the catalyst loading would lead to a change in efficiency, and there's a positive correlation between the concentration of the photocatalyst and its activity [39]. However, there is an optimum loading level for the quantity of photocatalyst after which the activity reaches a plateau, excess catalyst would block the penetration of light into the solution, resulting

in an unfavorable light scattering [40]. It is important to load a suitable amount of catalyst [41].

1.2.3 Concentration of the substrate

The efficiency of photocatalyst is also affected by the concentration of organic substrate, because when activity sites on the photocatalyst surface become saturated over a high concentration of substrate, there would be no enough activity sites for excess substrate, leading to an unfavorable decrease on the photocatalyst efficiency [42].

1.2.4 Intensity of light

It has been reported that as the intensity of light increases, the degradation rate of substrate increasing, which means the radiation absorption of photocatalyst play an important role on the efficiency of photoreaction [43-45].

1.2.5 pH level

The pH in a solution is a very important factor for the photocatalysis efficiency [46]. The pH of the medium to be treated not only affects the surface charge properties of the photocatalyst, but also the size of agglomerates which are formed on the particular surface sites of photocatalyst during the photocatalytic reaction [47]. It has been reported that there should be a support for organic pollutants degradation if there is an optimum environment [48].

1.2.6 Temperature

Temperature is another factor that might influence on photocatalytic activities, the reason

probably is the increasing temperature enhances the recombination chance of electron-holes, as well as the desorption of absorbed species that formed on the surface of the photocatalyst [49]. The results can be described by Arrhenius equation as shown following:

$$K=Ae^{-Ea/(R*T)}$$

Where K represents the Rate constant, A represents the pre-exponential factor, Ea represents the activation energy and R represents the universal gas constant.

1.3 Introduction to Tungsten Oxide (WO_3)

TiO_2 is the most widely studied photocatalyst since a long time, it has many merits such as photo-stability, inert nature (chemically and biologically), it is cost effective, etc. TiO_2 can only perform under ultraviolet (UV) light (3% of full spectrum light), and barely work under visible light (44% of full spectrum light), which means it wastes the majority of the solar energy. Recently, WO_3 is getting more and more attention as a promising, effective and visible-light-harvesting photocatalyst.

1.3.1 Structure of WO_3

The crystal structure of WO_3 is temperature and process dependent. It has several different polymorphs:

Table 2: Different phases of WO_3 under different temperature [50]

Temperature (K)	Phase
230	Triclinic
300	Monoclinic
623	Orthorhombic
900	Tetragonal

Among all these structures, the most common one is monoclinic with space group P21/n [51].

The figure 3 below shows a Crystal structure of tungsten (VI) oxide:

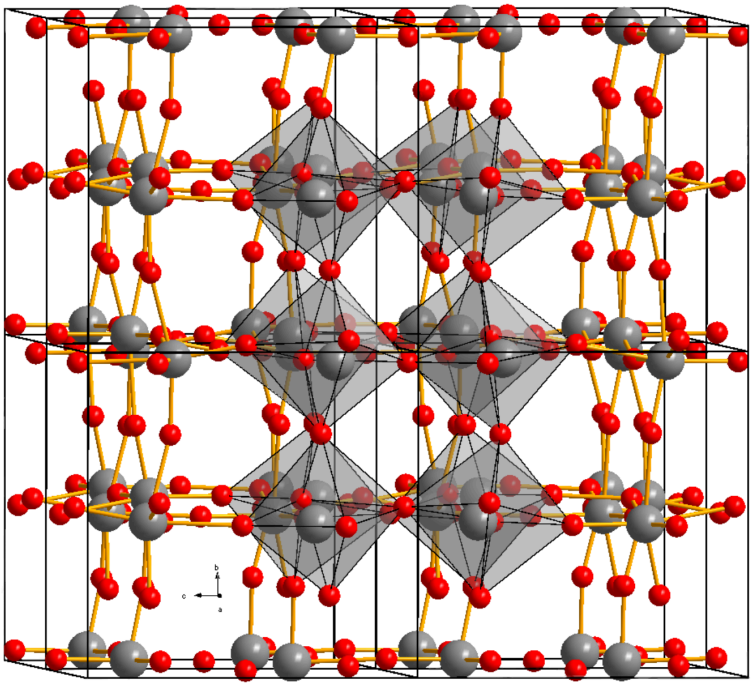

Figure 3: Crystal structure of tungsten (VI) oxide [52]

WO_3 is one of the n-type metal oxide semiconductors, with a band gap energy of E=2.7eV (for the monoclinic phase), which means that WO_3 has visible light scale absorption edge [53-54]. There have been many reports shown that WO_3 can be successfully used in

photoelectrocatalystic process [55-56], such as electrocatalysis [57], gas sensor [58-59], and electrochromic devices [60-62]. WO_3 can be produced via several different processes, like sol-gel methods, sputtering thermal evaporation and many others. Besides, there are great efforts have been explored for synthesizing WO_3, nanostructures like nanopowders, nanorods, nanowires, nanofibers, nanoparticles, etc [54].

1.4 Introduction to Polyaniline (PANI)

Polymers were regarded as insulator for a long time, but since 1976, chemist Mac Diarmid from University of Pennsylvania with his research group firstly discovered that doped polyacetylene had properties similar to a metal, which aroused enormous attention on polymers' structure and formation, leading to a new field, that of conducting polymers. In subsequent studies, polyaniline (PANI), Polypyrrole (PPy), and Polythiophene (PTs) and many other conducting polymers were explored [63]. Conducting polymers become important materials and attract many attentions in recent years as the most advanced materials in many modern industries, such as biosensors [64], electrochemical capacitors [65]. So it has great practical value studying on conducting polymers.

Among all the conducting polymers, polyacetylene is one of the earliest and deepest studied conducting polymers, but the preparation conditions for polyacetylene are very strict and its lack of environmental instability puts many obstacles for its application. PANI enjoys cost efficiency, simple preparation, good inoxidizability and high temperature resistance, excellent chemical and electrochemical stability, it is easy to fashion as film, it shows electrochromic properties and large capacitance, etc [14-16], Thus it is one of the most promising conducting polymers.. Even though MacDiarmid group developed PANI just in 1984, PANI became one of

the most popular conducting polymers in the world. Since then many researchers have been studying widely on structure, character, doping, modification and so many other areas.

1.4.1 Structure of PANI

MacDiarmid pointed that PANI probably could be a head-tail structure of linear polymer based on the study on ^{13}C-NMR and IR, which is made of benzene ring and quinone ring alternative structure, but this structure is inconsistent according to recent experiment data. In 1987, MacDiarmid reported a structure that been widely accepted, which consists of Benzenoid diamine and Quinoid diimine, these two units can become reversible through redox process:

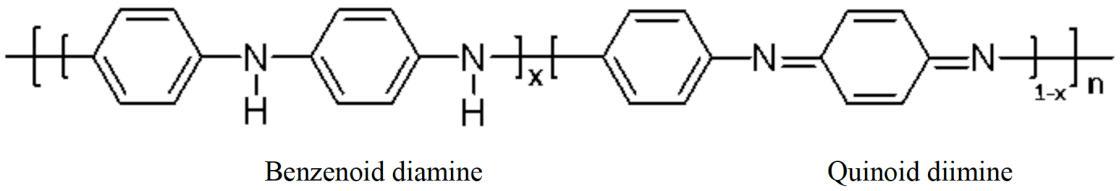

Benzenoid diamine Quinoid diimine

Figure 4: Structure of PANI with two units [66]

In the figure 4 shown above, x is the value to represent redox level, different x relate to different contracture, composition, and conductivity. When x=0, it is a completely oxidized form that is called Pernigraniline; when x=1, it is a completely reduced form that is called Leucoemeraldine; When x=0.5, it is a semi-oxidized form that is called Emeraldine. x=0(Pernigraniline) and x=1(Leucoemeraldine) are both insulator, but when 0<x<1, PANI become a conductor, and when x=0.5 (Emeraldine) PANI has the best conductivity. The following figure 5 shown three oxidation reversible forms [67]:

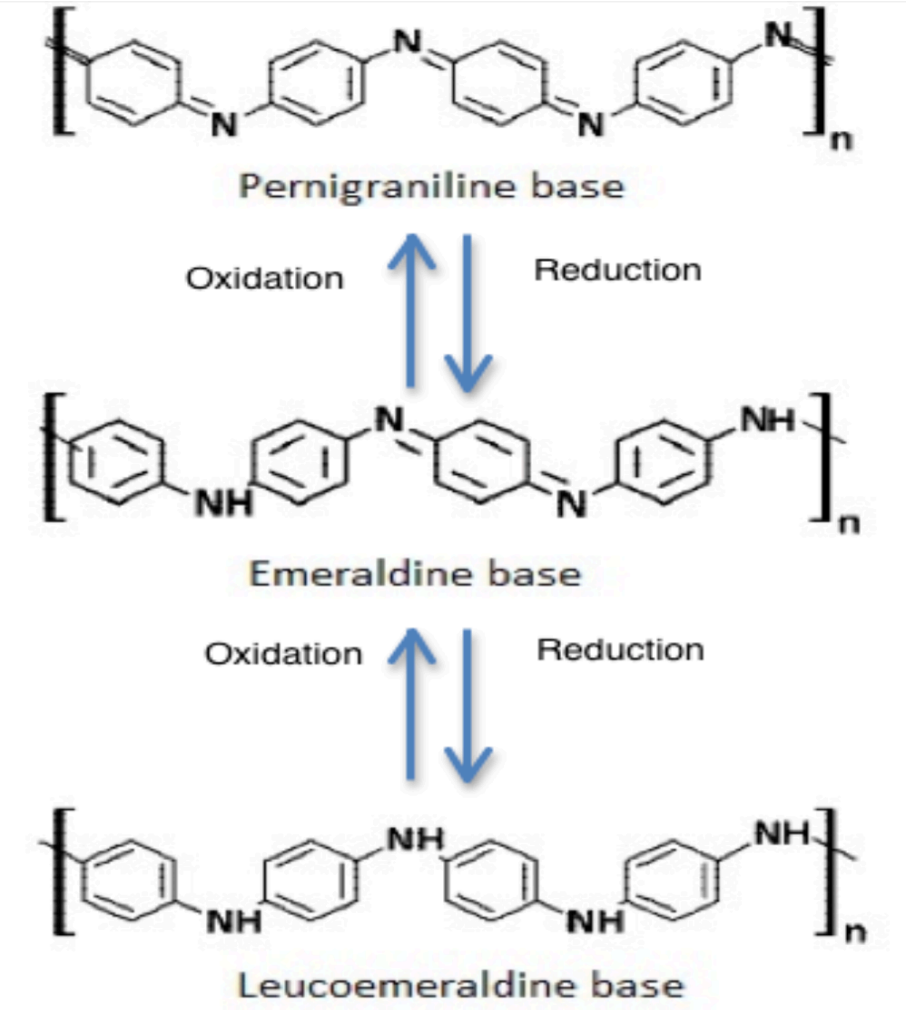

Figure 5: Reversible redox reaction of PANI [66]

1.4.2 Doping mechanism of PANI

PANI is a conjugated polymer that consists of alternative single and double bones along the backbone. There is a localized strong σ bond in each pair of single and double bones and a weak π bone in every double bone. However, this conjugated structure is too weak to support charge transfer, thus doping is needed to import charge carriers into PANI. These carriers could be holes or extra electrons. One useful method is to introduce hydrochloric acid to bring with the PANI, through which H^+ can "act" as the holes. When an electron moves to an adjacent spot, a

hole will be occupied and at the same time a new hole is formed. This continuous occupied and created holes pattern will allow the charges to move for a long distance along the backbone [68]. The figure 6 below shown the doping process of PANI with HCl:

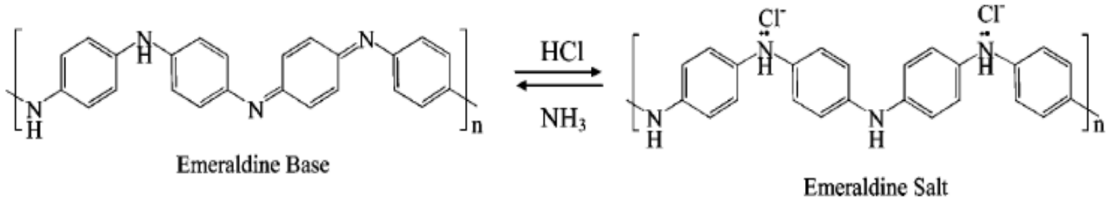

Figure 6: PANI emeraldine base doping with HCl [69]

1.4.3 Solubility of PANI in some common organic solvents

Since 1970 many syntheses method for PANI have been introduced [70-71], yet there has not been much development on the solubility of PANI. Genies had reported that PANI couldn't be dissolved in most organic solvents no matter what the preparation methods are used [72]. Wang also reported that PANI could partly or completely dissolve in chloroform, THF, NMP and some other organic solvents [73]. The table 3 below shown some organic solvents that can partly or completely dissolve PANI:

Table 3: The solubility of PANI in different solvents [74]

Solvents	Sample/ Solvent (g/ ml)	Concentration (g/ ml)	Percent of solute (%)	Colour of solution
NMP	0.25/25	9.2×10^{-3}	92	dark blue
DMAC	0.25/25	8.4×10^{-3}	84	dark blue
DMF	0.25/25	6.4×10^{-3}	64	dark blue
DMSO	0.25/25	4.4×10^{-3}	44	dark blue
THF	0.25/25	1.2×10^{-3}	12	dark blue
Chloroform	0.25/25	1.0×10^{-3}	10	brown
Toluene	0.25/25	3×10^{-4}	3	light yellow
Acetone	0.25/25	2×10^{-4}	2	light yellow

From the solvents shown above, we can tell PANI can only be dissolved in limited

solvents that are either toxic or not environment friendly, so these solvents are not good options for synthesizing composite photocatalysts cause we need to make environmental friendly material instead of some ones can bring secondary pollution. So in this project, we don't use any toxic solvents to dissolve PANI in a chemical way, instead we use a physical way, which will be cleaner and nontoxic.

1.5 Potential advantages of WO_3/PANI composite film

In recent years, environment pollution and energy problems bring more and more attention to the need of photocatalytic remediation. Photocatalysis is one of the most useful methods to solve above problems based on photocatalytic degradation pollution and photocatalytic hydrogen making. Among all kinds of photocatalysts, WO_3 enjoy many merits and has a lower band gap, it is believed one of the most promising semiconductor photocatalyst; PANI as one of the most important conducting polymers enjoy many properties, it contains π bond that is constructed by parallel p orbitals, leading to PANI can easily react with other chemical bonds and has good photoelectricity. Besides, PANI has good electrons transfer property, which will make a contribution to improving photoelectrons separation efficiency in order to improve the photocatalytic activities on WO_3, and its holes transfer property will decrease the photocorrosion.

In additional, in this project I make this hybrid material into a thin film, which will not only improve the reaction area, but also make it very easy to recycle and won't bring secondary pollution.

1.6 The matrix of Cellulose Acetate

In this project, I introduce Cellulose Acetate (CA) as the matrix for WO_3 and PANI for preparing the hybrid thin film. The reasons that choose CA as the matrix are: first, PANI and WO_3 are both very hard to be dissolved in solvents, so we need CA solution which enjoys good viscosity to make them disperse well and evenly in order to connect them into films; Second, the structure and high intermolecular form of CA let it have a high degree of crystallinity [75-76], which can let CA as a matrix, combine with other conducting polymers like PANI to provide holes for transferring charges. In this project, CA plays a role as holes transferring layer for PANI [77]; Third, CA is a environmental friendly materials enjoys the properties such as, good biocompatibility, nontoxic, colorless, tasteless and low cost [78]; Besides, CA is hydrophobic polymer that will make the composite film an easy to preparation and recycle. All in all, CA is an optimum matrix material for WO_3/PANI composite film preparation. The figure 7 shown below is the molecular structure of CA:

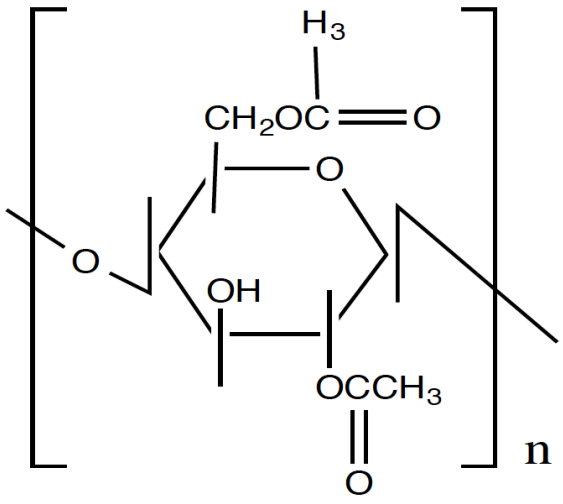

Figure 7: Molecular structure of Cellulose Acetate [66]

It has been reported that CA as matrix used for organic and metal materials. Liu [79] has

reported that CA as matrix for Graphene, making the Graphene dispersed evenly to generate a thin film and to enhance the film's mechanical property; D. Chen [80] has also reported that the combination of CA and gold to make a glucose biosensor, CA immobilized the matrix and had a good support for the composite.

1.7 Spin coating

Spin coating is a very useful and common method to get uniform thin films on flat substrates. The following figure 8 briefly shown the procedures of how spin coating works:

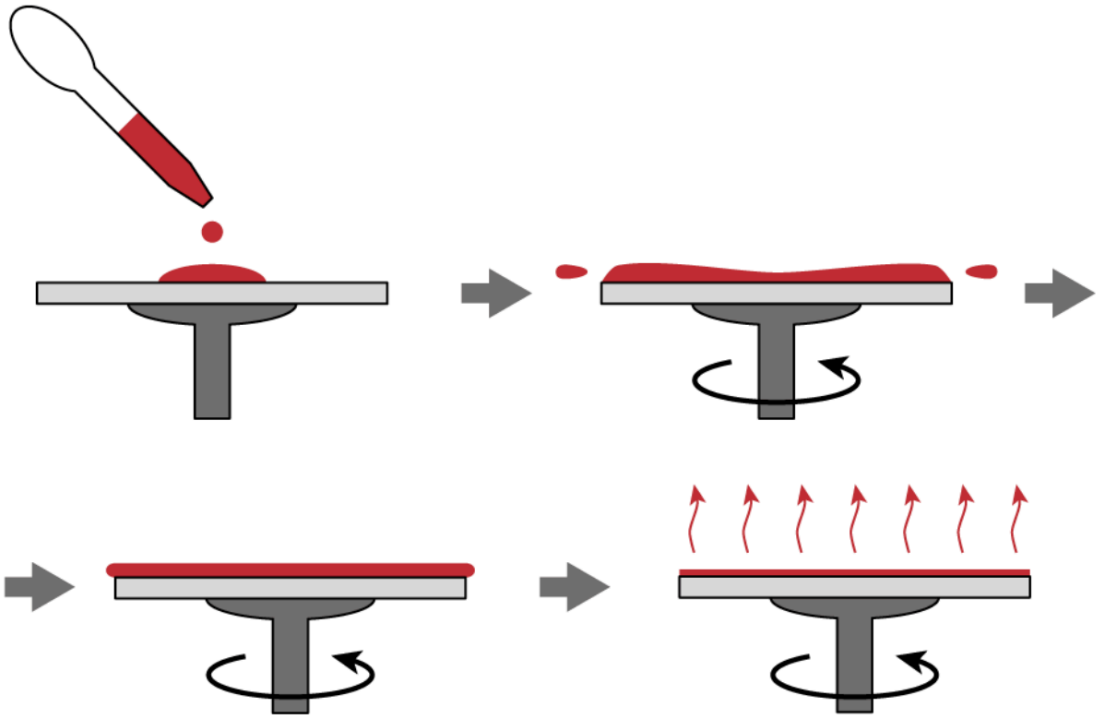

Figure 8: The brief procedures of spin coating [81]

From the figure 8 shown above, the first step of spin coating is to put a small amount of prepared coating material onto the center of the substrate, at the same time the substrate is not

spinning or keep at a low speed spinning (top left); Secondly, the substrate is turned up to higher speed so that the coating material can get enough centrifugal force to spread out, meanwhile don't forget to close the lid of the spin coating machine in case of spilling out (top right); thirdly, adjust the substrate speed to decrease the film thickness and make the coating materials dispersed well and evenly (bottom left); Finally, keep the substrate under a stable spinning speed while the solvent evaporates (bottom right).

1.7.1 Parameters that affect spin coating

There are several parameters that influence on the thickness and uniformity of the coating materials. The figure 9 shown below illustrate some main factors:

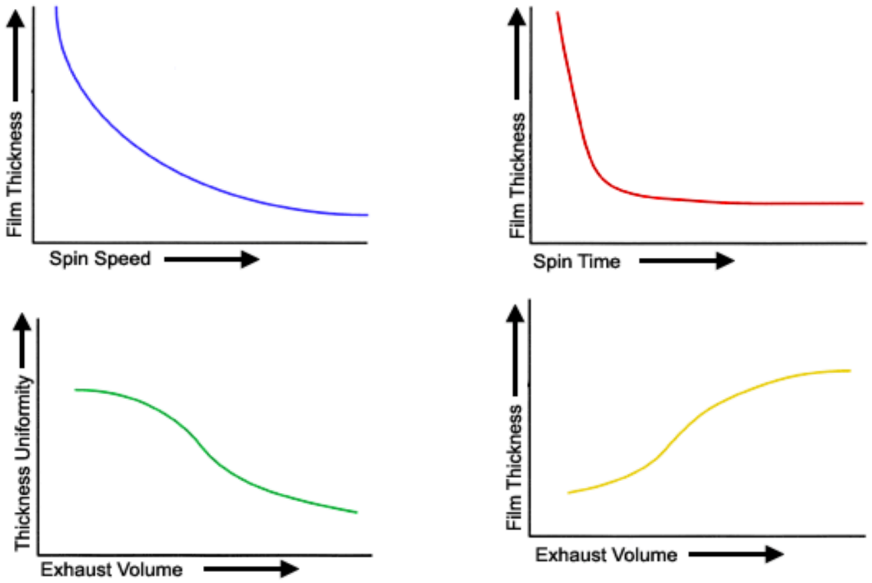

Figure 9: Some factors that affect spin coating materials (Source: Brewer Science Inc)

Among all these parameters that decide the spin coating materials' properties, the viscosity and spin speed are two important ones.

The spin speed is dependent on the centrifugal force formula below:

$$F = mrw^2 = \frac{mv^2}{r}$$

Where F is the centrifugal force, w is angular speed and v is liner speed. From this formula we can tell a higher speed will result in a bigger centrifugal force, leading to thinner and more uniform film. Usually, the angular speed ranges from 1500rpm to 6000 rpm.

Besides, the solvent itself decides the viscosity. The higher viscosity of solution results of a higher viscous force so that it will need a higher speed to get coating film thinner and uniform.

1.8 Methylene Blue

Caro discovered the Methylene blue dye in 1878 [82], since then methylene blue has been studied for a long time and recent decades more and more researchers have used methylene blue as one of the most useful model dyes for testing the organic dye adsorption rate from substrate solution [83]. The following figure 10 shown the structure of methylene blue that consists of heterocyclic aromatic units:

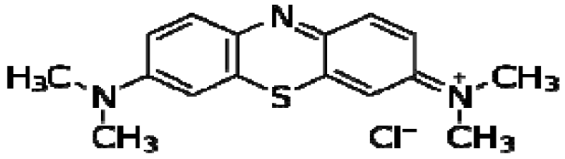

Figure 10: Methylene blue crystal structure [84]

Methylene blue dye has been widely applied in many areas such as textile, food, chemical and medical industries [85-86]. Methylene is used for dyeing wool, paper, silk even hair in textile industries; it is used as veterinarian antiseptic, peroxide generator and so on in chemical

area; it is also reported to be made to treat diseases in medical field such as psoriasis [87], cancer [88] and malaria [89], etc.

Even thought methylene blue can be used in many industries, it bring some negative effect, such as it will cause vomiting, shock, and even necrosis if contact for long time [90]. Besides, it is applied very commonly in dying industries, so the wastewater that contains methylene will be very dangerous. One of the most efficiency ways to treat the methylene including wastewater is to introduce photocatalyst, which can degrade methylene blue into small inorganic species [91-94], which is not harmful to environment and life. The following equation is using photocatalyst to break down methylene blue structure [95]:

$$C_{16}H_{18}N_3SCl + 25.5O_2 \rightarrow 16CO_2 + 6H_2O + 3HNO_3 + H_2SO_4$$

1.9 Salinity and sodium chloride

Salinity can be defined as the quantity of dissolved salt in water. There are many salts we can find in our life, such as sodium chloride, sodium bicarbonate and many others. The concept of salinity can be used in many areas, like oceans, lakes and rivers, the value of salinity depends on the salt dissolved in these fields, usually, ocean has biggest salinity, then the lake, and river has the smallest salinity. Besides, salinity also can be defined as the mass fraction, which means the dissolved mass of a unit mass in the solution. The table 4 below shows some salinity value for different water:

Table 4: The salinity value of different waters

Water	Salinity (g/kg)
Ocean	35
River and Lake	Less than 0.01 [96] to a few
Dead Sea	Around 200 [97]

Sodium chloride (NaCl) is one the most common salts in water. The figure 11 shown below is the crystal structure of NaCl:

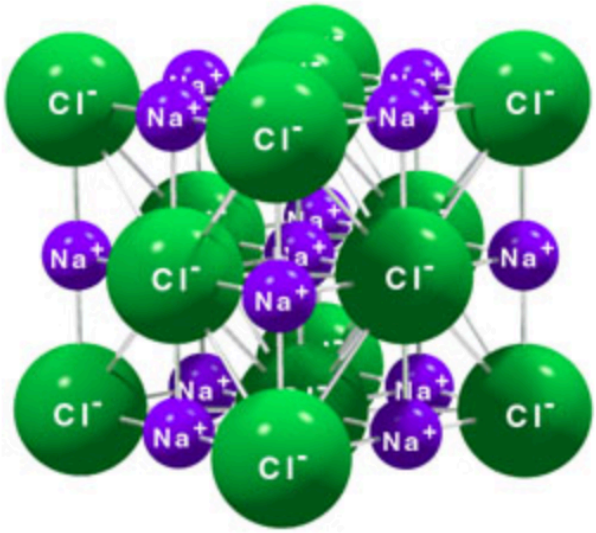

Figure 11: The sodium chloride crystal structure (Source: Washington University in St. Louis, 2005)

From the figure 11 we can tell the structure of NaCl is stereo symmetry, inside the crystal structure of NaCl, the bigger Cl^- arrange as cubic close packed, the small Na^+ fills the blank between the Cl^-; every ions are surrounded by other six ions. Many other compounds also use this structure of NaCl, which is called rock salt structure.

Due to the structure of NaCl, there is an interesting topic that if the exist of NaCl in water will affect the photolysis of Methylene blue, we did some experiments following to test different salinity influence on methylene blue photolysis.

Chapter 2: Materials Used

In this project, pure nanosized tungsten trioxide (nanopodwer<100nm particle size), polyaniline (emeraldine salt), cellulose acetate, hydrochloric acid, acetone and acetic acid are used to prepare the hybrid photocatalyst thin film; sodium chloride is used to test the photolysis of methylene blue solution. The table 5 below shows the chemicals used during this work:

Table 5: The properties of chemicals used to synthesize the photocatalystic film

Chemical Name	Chemical Formula	Molecular Mass (g/mol)	Density (g/cm^3)	Company
Tungsten (VI) oxide	WO_3	231.84	7.16	Sigma-Aldrich
Polyaniline (emeraldine salt)	$([C_6H_4NH]_2[C_6H_4N]_2)_n$	-	-	Sigma-Aldrich
Cellulose Acetate	$C_6H_7O_2(OH)_3$	~50,000	1.3	Sigma-Aldrich
Hydrochloric Acid	HCl	36.46	1.2	Sigma-Aldrich
Acetone	CH_3COCH_3	58.08	0.791	Pharmo-Aaper
Acetic Acid	CH_3COOH	60.05	1.05	Pharmo-Aaper
Sodium Chloride	NaCl	58.44	2.165	EMD Chemicals Inc.

Chapter 3: Methods of Preparation

There are several steps to synthesize the PANI/WO_3 and PANI/TiO_2 hybrid thin films, and these steps can be shortened to four sections: PANI doping, solution preparation, film synthesizing and film isolating from the matrix glass.

For the methylene blue solution photolysis part, I prepared four different salinity of NaCl solution.

3.1 Preparation of WO_3/PANI hybrid photocatalyst

3.1.1 Preparation of PANI (H^+)

10 ml HCl was carefully added to 0.1g PANI (EB salt) powders in a 20 ml vial overnight; then isolate the PANI particles by removing the top HCl, adding 10 ml DI water to wash PANI particles and centrifuging them to remove the top water, repeat the same procedures by 3 times DI water and 1 time acetone to get the H+ doped PANI.

3.1.2 Preparation of PANI(H+) and WO_3 solution

0.5g CA (Mn~50,000) was dissolved in acetone(2ml) and acetic acid(3ml) mixed solution, two sets of above solution were prepared in two vials, then ultrasound these two mixed solutions for 3 hours and keep them overnight to get the completely dissolved CA solution; put 0.1g PANI(H^+) into one solution and 0.1g WO_3 into another, then ultrasound these two solution for 1 hour to let the PANI(H^+) and WO_3 particles dispersed well and evenly in the solution.

3.1.3 Spin coating to get the WO_3/PANI thin film

Set up the spin coating machine for: T=40s and R=1500rpm; then spin coating these two solutions on a glass matrix separately to get a double layer thin film, the bottom layer is PANI and the upper layer is WO_3; put this as prepared thin film in fume hood for 6 hours to dry.

3.1.4 Film isolating from the glass matrix

After the double layer thin film became dry, put this matrix glass that the thin film stick with into a bigger beaker full with DI water, after several minutes, the film will float automatically and isolate from the matrix glass. The figure below shows the as prepared WO_3/PANI thin film:

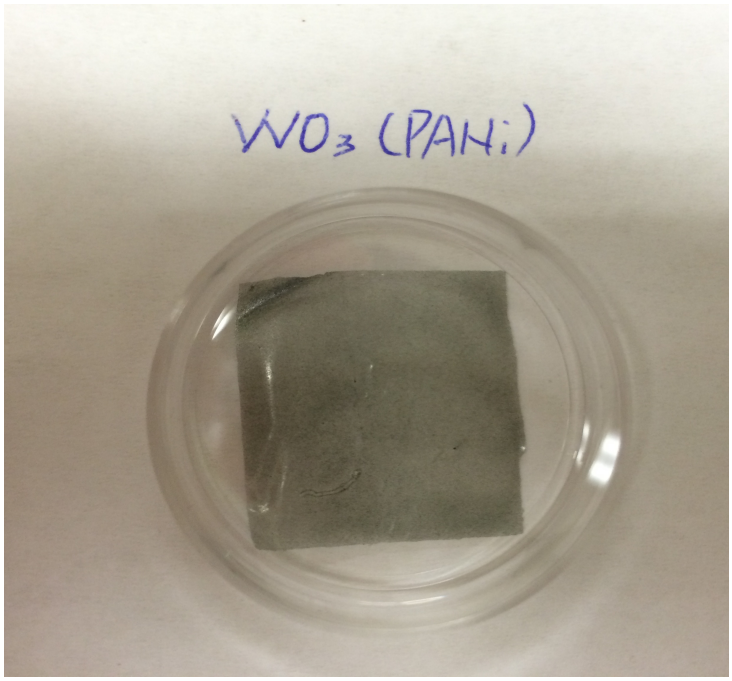

Figure 12: WO_3/PANI thin film

3.1.5 Preparation of TiO_2/PANI thin film

Titanium is believed one of the best metal oxide semiconductor materials for photocatalysis, so it's important to compare the degradation efficiency between WO_3/PANI and TiO_2/PANI, so I used the same method that prepared for WO_3/PANI film to synthesize TiO_2/PANI, except replaced WO_3 with TiO_2. The figure below shows the as prepared TiO_2/PANI thin film:

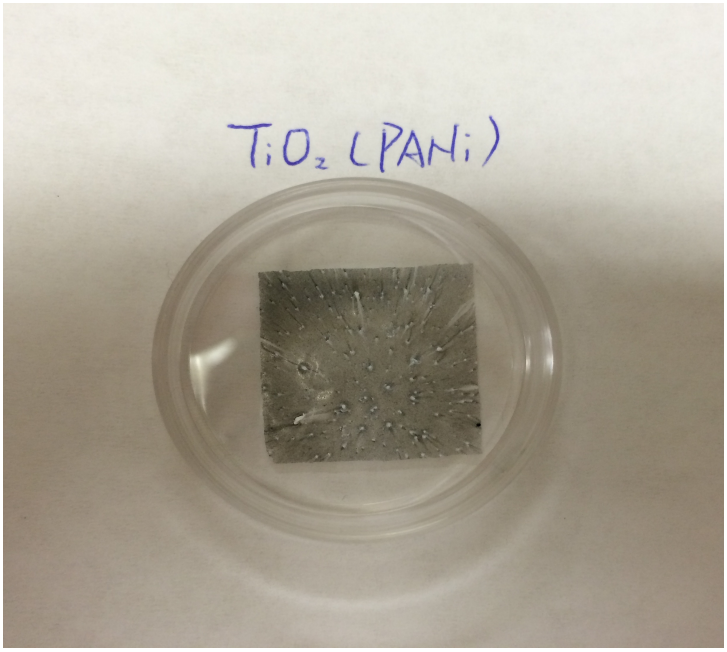

Figure 13: TiO_2/PANI thin film

3.1.6 Preparation of different salinity NaCl solution

Weighed 0.5g, 1.0g, and 1.5g NaCl particles and put them separately into three vials filled with 10ml DI water, and also prepare one vial just fill with 10ml DI water as a blank comparison. Then these four vials were ultrasound for 1 hour.

Thus, the WO_3/PANI thin film was prepared as methods described above, and then it was characterized by using SEM, EDS and TGA instruments. After characterization it was tested for its photocatalytic activity by adding methylene blue solution via UV-Vis facility and compare with TiO_2/PANI thin film and pure WO_3 under the visible light.

Besides, the four different salinity NaCl solutions were added methylene blue solution to test their photolytic activity under visible light by UV-Vis facility.

Chapter 4: Characterization techniques

4.1 Scanning Electron Microscopy (SEM)

In order to get more sample information from a microscopic level, we need the help from scanning electron microscopy, which is on the most useful instruments can be used for this purpose. The basic principle of SEM is using narrow electron beam that have very high energy to strike atoms of sample in order to produce signals that contain all kinds of information of the sample, such as sample's composition, topography and more other physical information.

In this work, a very tiny sample of WO_3/PANI thin film was used for SEM analyzing. Before SEM works we need to coat the sample with a thin gold layer, which is used to decrease the inference from noise signals. Then we put the gold-coated WO3/PANI sample into SEM chamber and make it fixed.

An LEO 1550 Schottkey Field Emission Scanning Electron Microscope was used to analyze the WO_3/PANI thin film with gold coating sample. We sued a back scatted signal with a 8mm work distance and 20 kV EHT to get all the images. Both sides of the film sample were scanned.

4.2 Energy Dispersive X-Ray Spectroscopy (EDS)

The Energy Dispersive X-Ray Spectroscopy (EDS) is a technique that used to obtain the elements' concentration of the sample. A high energy electrons beam strikes the sample and X-rays come out from the sample, we can get the sample's information by analyze the X-rays. An

element intensity image will show on the screen when a beam scanning on the sample. In this work, the LEO 1550 SEM is used to obtain the EDS information of the sample.

4.3 Thermogravimetric Analysis (TGA)

The Thermogravimetric Analysis is a device that used to measure the relation between the sample's weight as temperature increased or decreased. According to the change of sample's weight, we can get a curve on a computer that shows the mass ratio of the target compound that in the sample, and then analyze pertinent information of the materials. In this work, the WO_3/PANI sample was heated from 40 ^oC to 600 ^oC inside the TGA machine.

Photocatalytic Test

Photocatalytic tests were performed for WO_3/PANI thin film, TiO_2/PANI thin film and pure WO_3 powders. Photolysis tests were carried out for 0g, 0.5g, 1.0g and 1.5g NaCl solutions. Both photocatalysis and photolysis experiments were studied under visible light for their photocatalytic efficiency and photolytic rate separately. Methylene blue solution was used to analyze the photocatalytic efficiency and photolytic rate by observing its degradation rate every several minutes.

Before the photocatalytic experiment started, a 20ppm methylene blue dye solution was made by putting 0.1g methylene blue dye in 50ml water. 0.0164g WO_3/PANI film then was added to 5ml 20ppm methylene blue solution, keep it in dark overnight in order to get adsorption-desorption equilibrium. Before put it under visible light, 2ml sample solution was taken out to process an absorbance measurement in order to get a 0h absorbance value. Then put the sample solution under visible light for 3 hours and every hour 2 ml sample solution was pipetted out to test its absorbance intensity via a facility called spectrophotometer. During this work, the visible light source is supported by a Newport ultraviolet light source with a 60W light bulb, and the settings of this source are 15A, 20V, and total power is 300W; the measurement is made by the spectrasuite software; and the wavelength of absorbance vale for measurement during this experiment is 655nm.

For the photolytic experiment test, 0g, 0.5g, 1.0g and 1.5g NaCl was dissolved in 10ml DI water and ultrasound for 1 hour till all NaCl completely dissolved in the DI water, then 2ml 25ppm(0.1mg methylene blue dye in 40ml DI water) was added to these NaCl solutions. The four vials were put under visible light for 3 hours and measurement method is the same with

photocatalytic test, and the settings of the light source are 10A, 20V, and total power is 300W, and the wavelength of absorbance value is 665nm.

4.4 Ultraviolet-visible Spectroscopy (UV-vis)

The Ultraviolet-visible Spectroscopy is a very useful technique to measure the loss intensity in a beam after it passing through a test sample. The facility used for UV-vis spectroscopy test is called UV-vis spectrometer, which usually includes a light source that used to produce visible or ultraviolet light, a diffraction grating that used to separate the wavelengths of light, a sample holder to fix the sample and a detector to get the information of the reflected or absorbed light. The figure 14 shown below is a set-up of spectrometer:

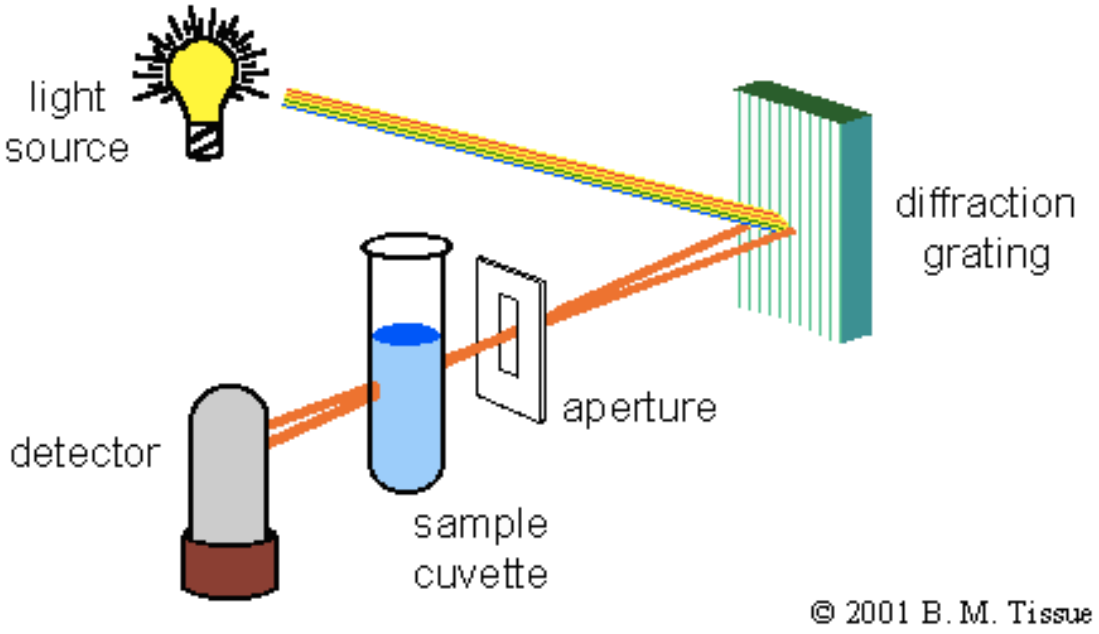

Figure 14: UV-vis spectrometer set-up (Source: 2001 B.M Tissue)

In this project, an Ocean Optics model HR 4000 is used as the spectrometer, it contains a deuterium and halogen lamp for UV and visible light respectively, and it comes along with an analysis software is called SpectraSuite.

The functions of the spectrometer contain absorbance spectrum and transmittance spectrum. Before the light pass through the sample cuvette, its intensity is recorded as I_o, and I is recorded as the intensity of the light passed through the sample cuvette. The equations shown below are for Transmittance spectrum(T) and Absorbance spectrum(A) (Source: SpctraSuite Installation and Operation Manual, Ocean Optics, Inc):

$$\%T=(S-D/R-D)*100\%$$

$$A=-\log (\%T/100\%)$$

Where S is the sample intensity at wavelength λ, D is the dark intensity at wavelength λ, and R is the reference intensity at wavelength λ.

Chapter 5: Result and Discussions

5.1 Characterization with SEM with EDS

In order to analyze the morphology of both sides of the WO_3/PANI double layer film, SEM images at 300x and 1.00kx are taken. The settings are: walking distance is 8mm; EHT is 20.00kV and backscattered single.

As shown in figure 15 below, image (a) and (b) are upper layer (WO_3 layer), from which we can tell the WO_3 particles are dispersed well and evenly on the PANI layer. From image (3) and (4) we can tell the bottom layer are PANI layer and without WO_3 particles. The WO_3 is like the "toppings" dispersed well on the PANI "Pizza".

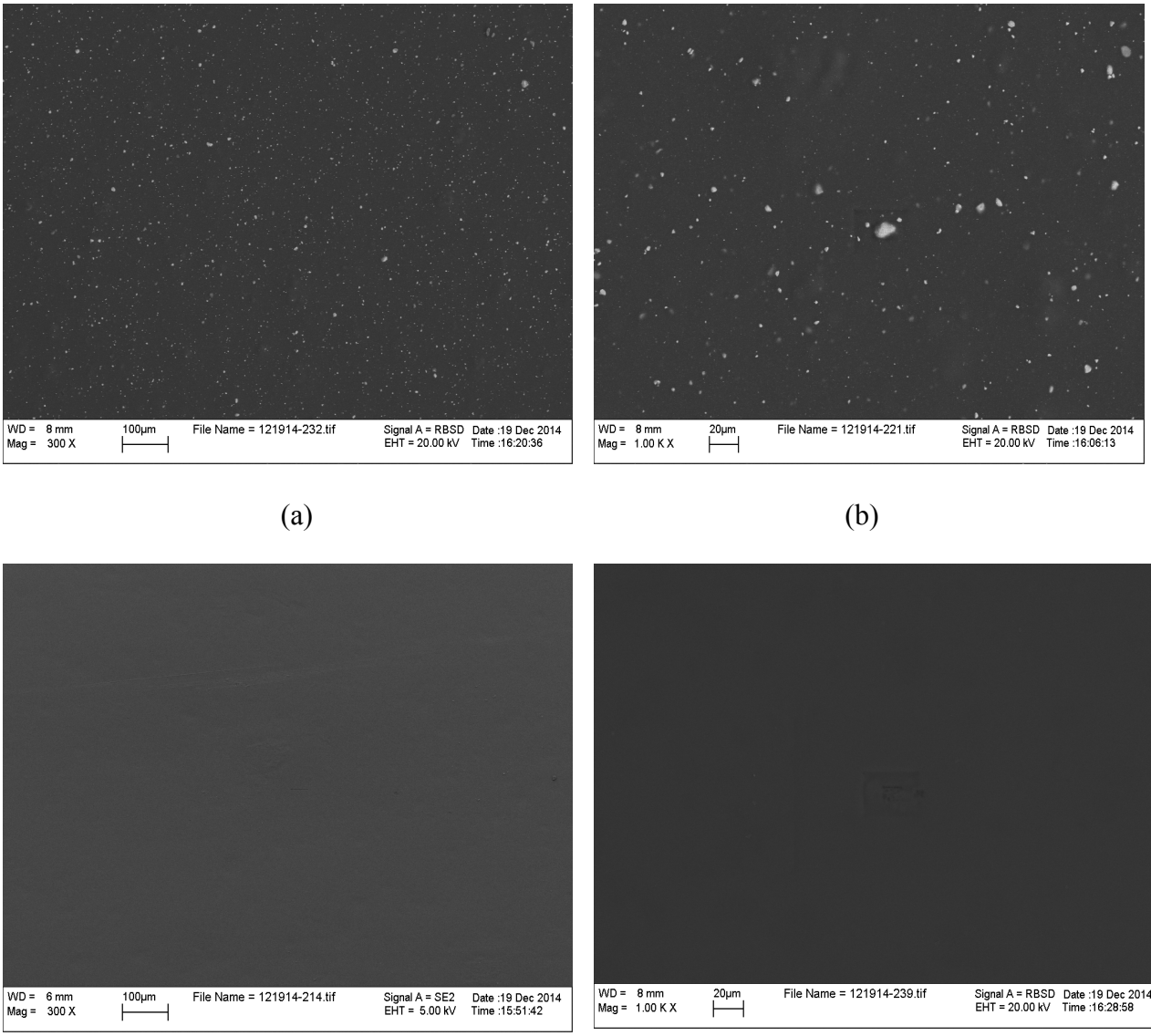

Figure 15: SEM images of (a)upper layer at Mag=300x; (b)upper layer at Mag=1.00kx; (c) bottom layer at Mag=300x; (d)bottom layer at Mag=1.00kx

From the EDS spectra image show below, we can tell the tungsten is well doped on the PANI layer with CA matrix.

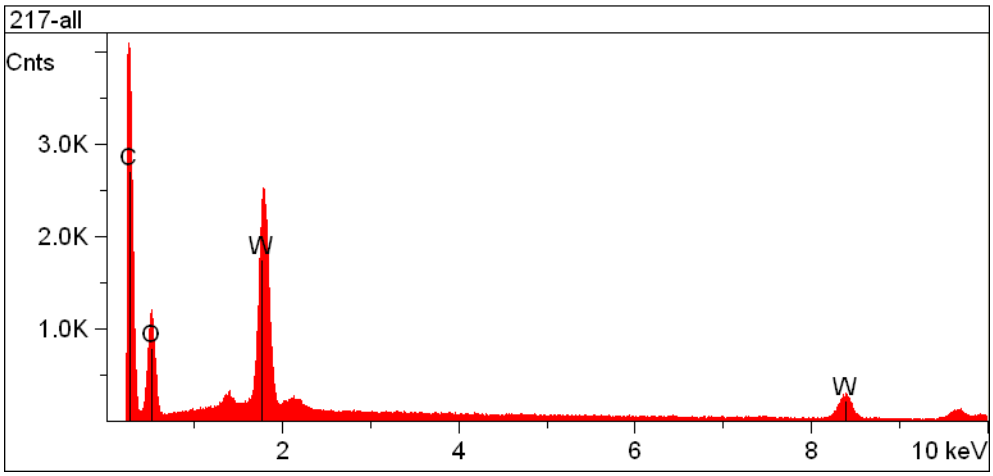

Figure 16: EDS of the WO_3/PANI film

5.2 Characterization using Thermogravimetric Analysis (TGA)

The thermogravimetric is used to analyze the weight ratio of each composition in the sample. The figure 17 show below is made of the weight and temperature, from which we can tell there are three inflection points, the three points are around 210 ^{o}C, 240 ^{o}C and 530 ^{o}C, which means there are three compositions started to disappear during from these points, according to the melting points of Cellulose Acetate and PANI are around 230 ^{o}C, 300 ^{o}C respectively, and around 550 ^{o}C part of WO_3 start to sublimate [98]. In addition, the point of 240 corresponding to around 60% weight of the sample, point of 530 corresponding to around 20% weight of the sample, so we can get the idea that the weight ratio of the CA, PANI and WO_3 are around 60%, 20% and 20% respectively. In this work, 0.0164g WO_3/PANI thin film was used to test for methylene blue degradation under visible light, in order to compare WO_3 photocatalytic

activity before and after compositing with PANI, 0.0033g WO_3 (20% weight of tested WO_3/PANI film mass).

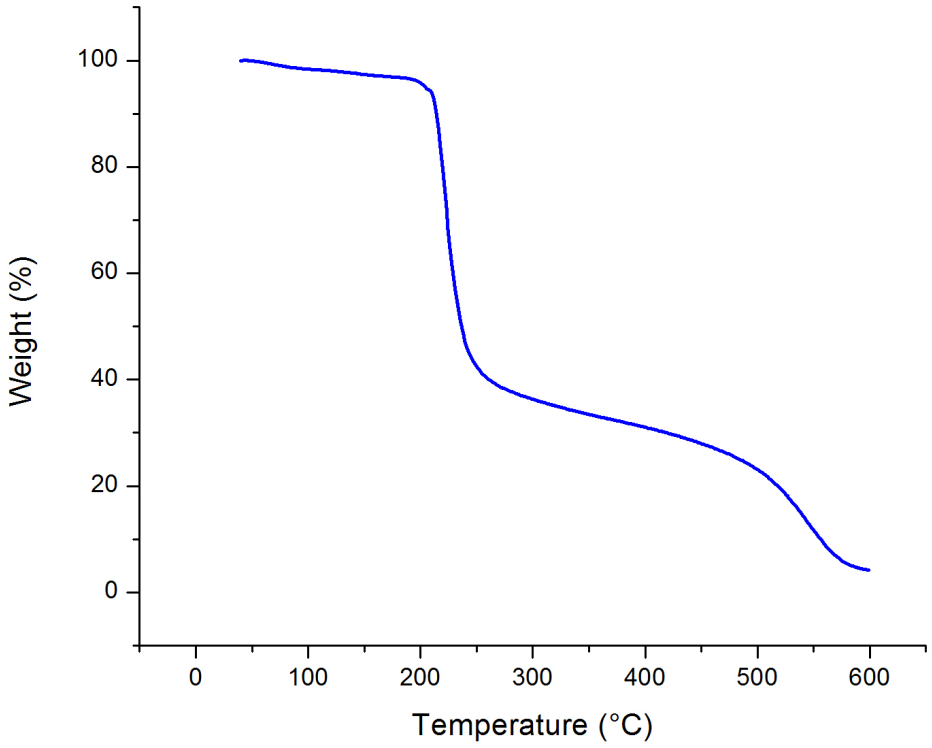

Figure 17: TGA analysis of WO_3/PANI film

5.3 UV-vis Spectroscopic Analysis

The synthesized WO_3/PANI thin film and TiO_2/PANI thin film along with WO_3 were tested by adding to methylene blue solution to check the degradation of the methylene blue under visible light. The absorbance value was recorded at a wavelength of 655nm for each measurement.

At the beginning of the test, 0.0164g of the WO_3/PANI, TiO_2/PANI and 0.0033g pure WO_3 were added to a 5ml, 20ppm methylene blue solution in vials respectively, then keep these

three vials in dark over night (about 12 hours) in order to get an adsorption desorption equilibrium between photocatalysts and methylene blue. After one night, these three vials are taken once absorbance measurement and recorded the value as 0 minutes reference and immediately kept under visible light to check the efficiency of these photocatalyst by recording the absorbance value every hour and totally for 3hours. Four different time plots were made in the same graph by using intensity value against wavelength. The peak intensity for these plots is at 655 nm.

5.3.1 Absorbance graphs for visible light degradation

Figure 18 below shows the degradation of methylene blue solution with WO_3/PANI photocatalyst under visible light. According to the analysis of this plot, which shows that before the visible light illumination the absorbance value is 1.502 and it gradually decreased to 0.117 after three hours illumination. After calculating the degradation percentage of methylene dye at the end of three hours is about 88.3%.

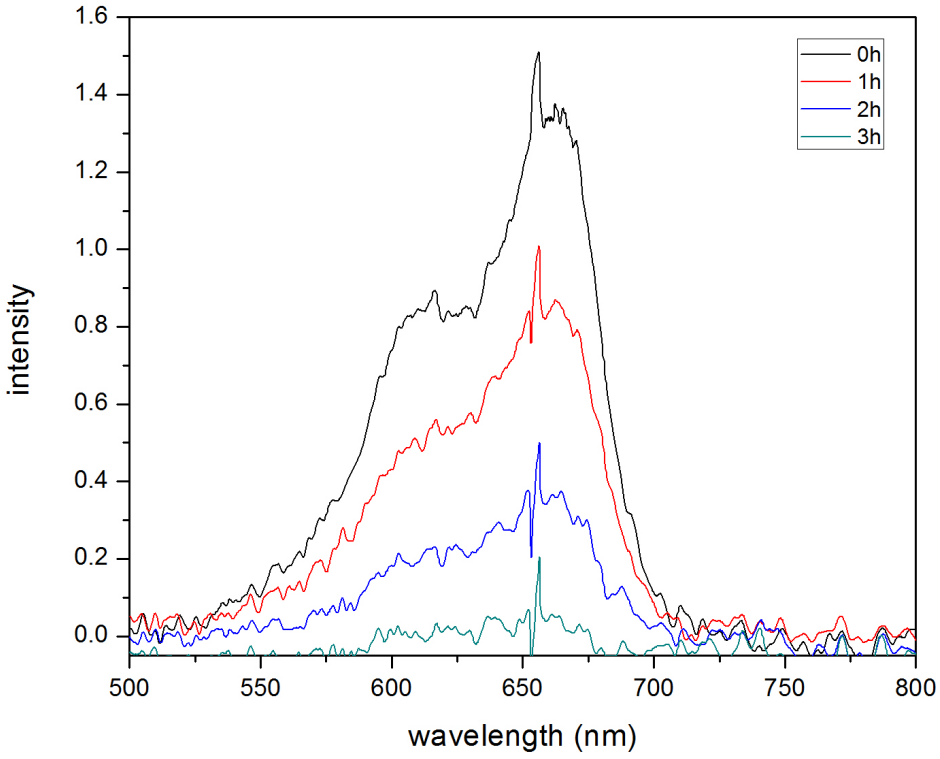

Figure 18: Graph of absorbance intensity versus wavelength for WO_3/PANI film under visible light

The figure 19 below shows the degradation of methylene blue solution with TiO_2/PANI photocatalyst under visible light. It shows that the methylene blue degradation at 180 minutes is lesser than that for WO_3/PANI (figure 18). The final degradation of methylene blue dye at the end of 3 hours is 39.1%.

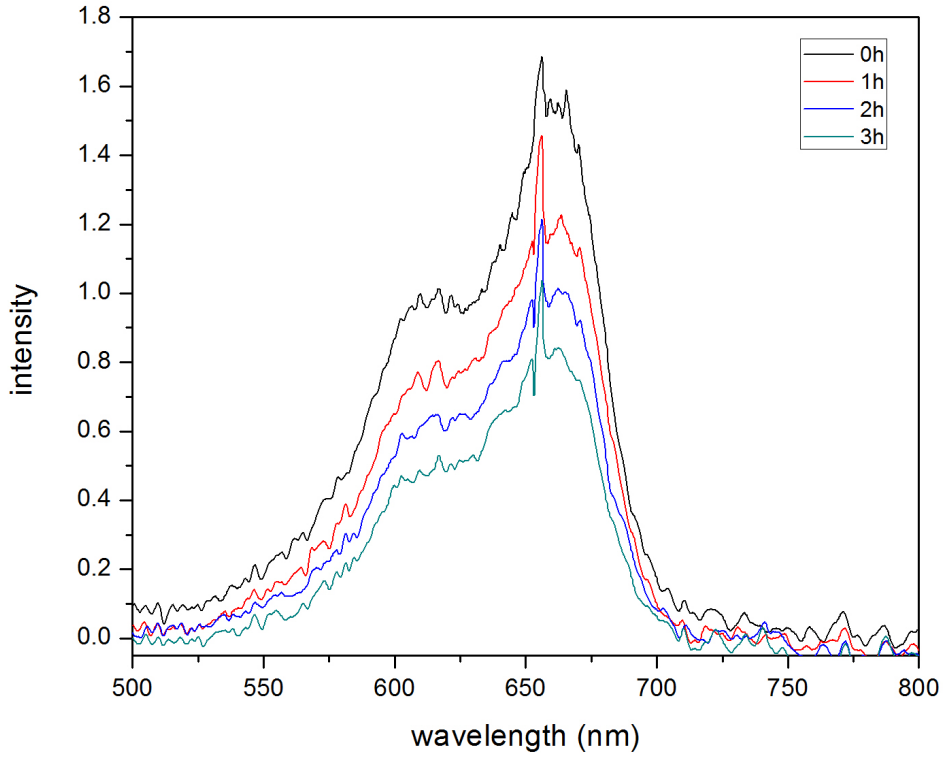

Figure 19: Graph of absorbance intensity versus wavelength for TiO_2/PANI film under visible light

The figure 20 shows the degradation of methylene blue solution with pure WO_3 under visible light. From the graph we can clearly tell that the degradation of methylene blue solution at 180 minute is more than that for the TiO_2/PANI (figure 19) film but less than that for WO_3/PANI (figure 20) thin film. The final degradation of methylene blue dye at the end of 180 minutes is 62.4%.

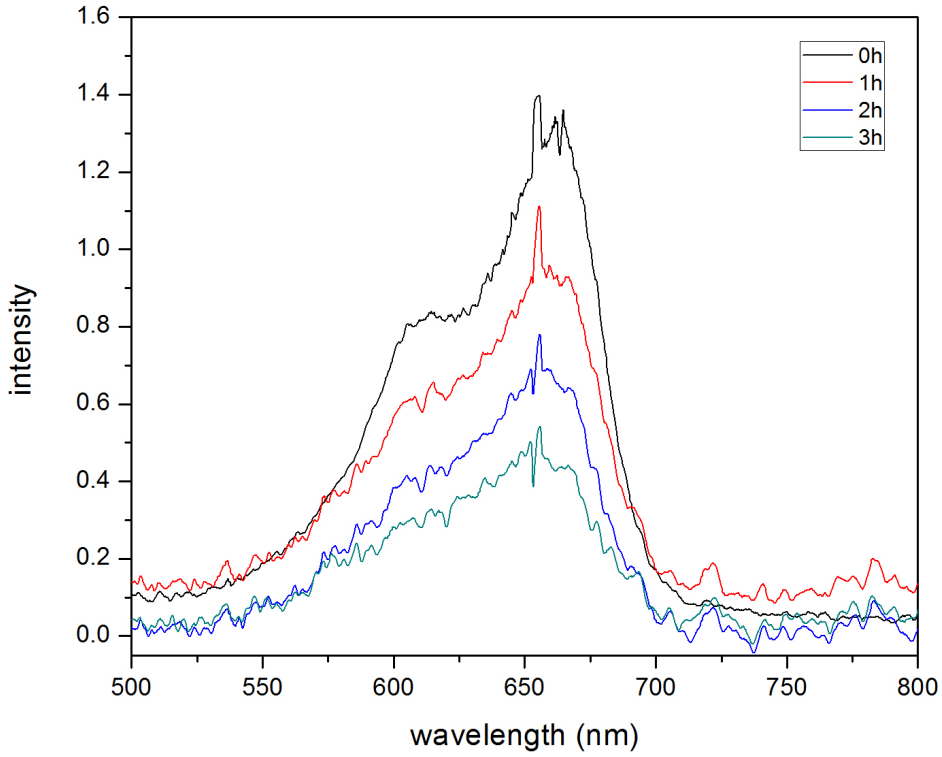

Figure 20: Graph of absorbance intensity versus wavelength for WO_3 under visible light

The Table 6 below shows the degradation percentage for the three catalysts at a time of 180 minutes.

Table 6: Degradation percentage of catalyst under visible light at 180 minutes

	WO_3/PANI film	WO_3	TiO_2/PANI film
Irradiation Time (minutes)	180	180	180
Percentage Degradation	88.3%	62.4%	39.1%

5.3.2 Comparative analysis of degradation under UV light

In order to better compare the degradation of methylene blue for these three photocatalyst under visible light. The figure 21 below shows the absolute value of absorbance intensity C/C_o (Y-axis), which means the percentage of the absorbance value at time C to the one at time C_o=0 minute, changing as the time (X-axis) increases up to 180 minutes.

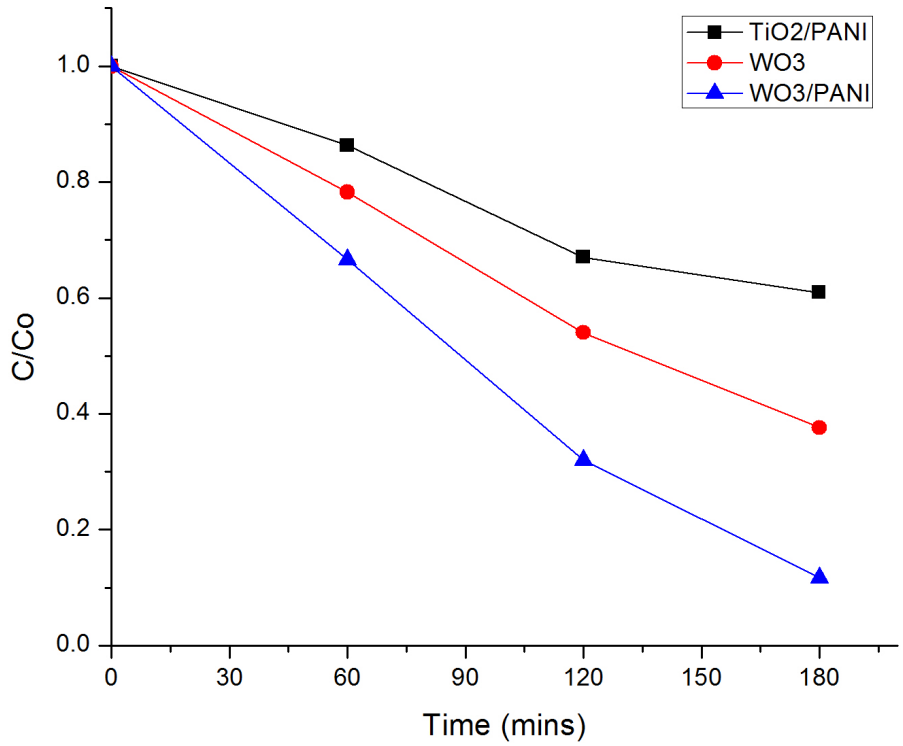

Figure 21: Graph of the degradation of the three photocatalysts under visible light

Therefore, from the comparison for these three photocatalyst shown above in figure 21, it can clearly tell that the WO_3/PANI have a good photocatalytic activity under visible light.

5.4 Methylene Blue Solution Photolytic Analysis

The methylene blue solution photolysis experiments were taken by adding 0.5g, 1.0g, 1.5g NaCl particles into 10 ml DI water with 2ml 25ppm methylene blue solution, and a 10 ml DI water with 2 ml 25ppm methylene blue solution without NaCl was used as reference. The Figure 22 below shows the pH value of these four samples:

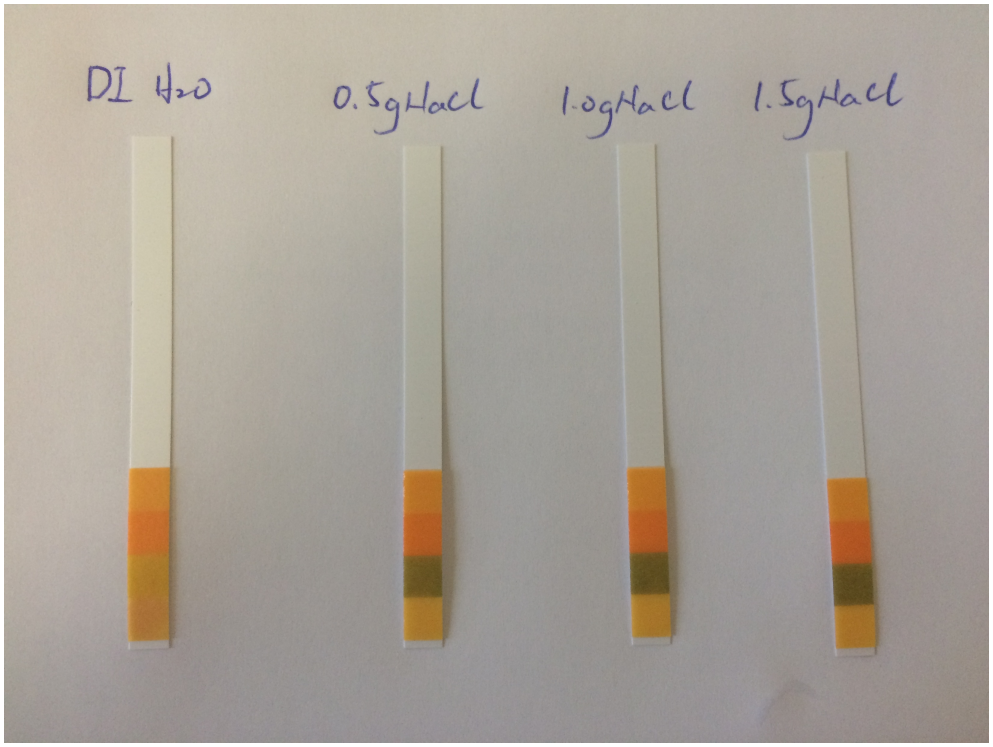

Figure 22: The pH test for four samples

After comparing to the pH standard value with all these three samples, the one without NaCl has a pH value around 5, the one with 0.5g NaCl has a pH value around 6, the one with 1.0g NaCl has a pH value around 6.5 and the one with 1.5g NaCl has a pH value around 7.

5.4.1 Absorbance Graphs for photolytic degradation

The figure 23 below shows the degradation of methylene blue solution without NaCl under visible light. After 180 minutes the degradation of methylene blue dye is 32.2%.

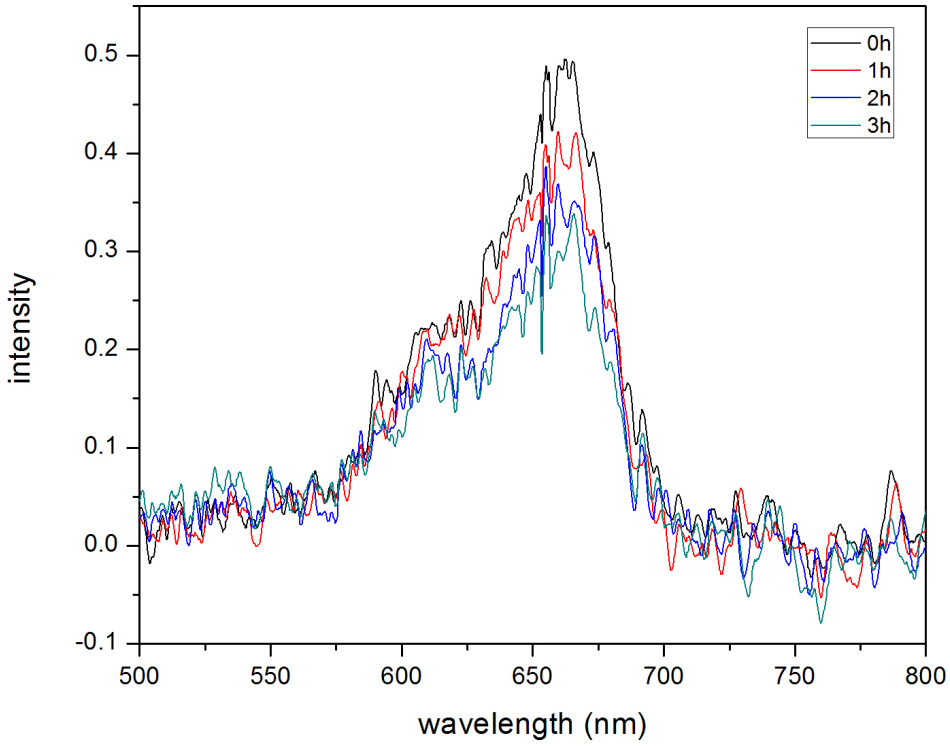

Figure 23: Graph of absorbance versus wavelength for 0g NaCl methylene blue solution

The figure 24 below shows the degradation of methylene blue solution with 0.5g NaCl under visible light. After 3 hours, the degradation of methylene blue dye is 18.2%.

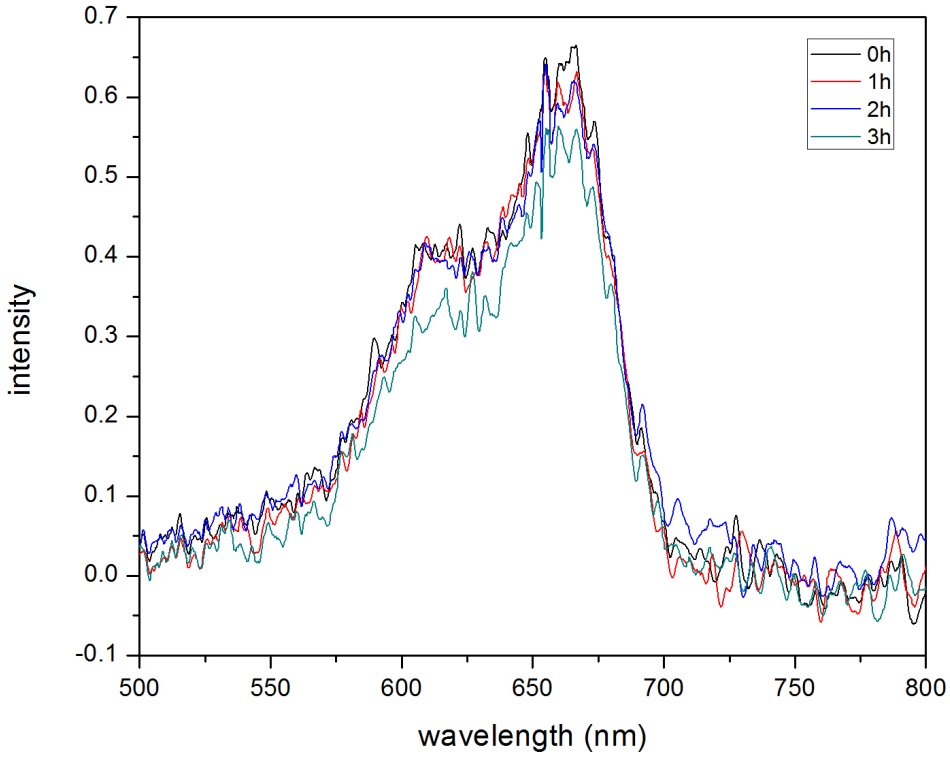

Figure 24: Graph of absorbance versus wavelength for 0.5g NaCl methylene blue solution

The figure 25 below shows the degradation of methylene blue solution with 1.0g NaCl under visible light. After 3 hours, the degradation of methylene blue dye is 16.6%.

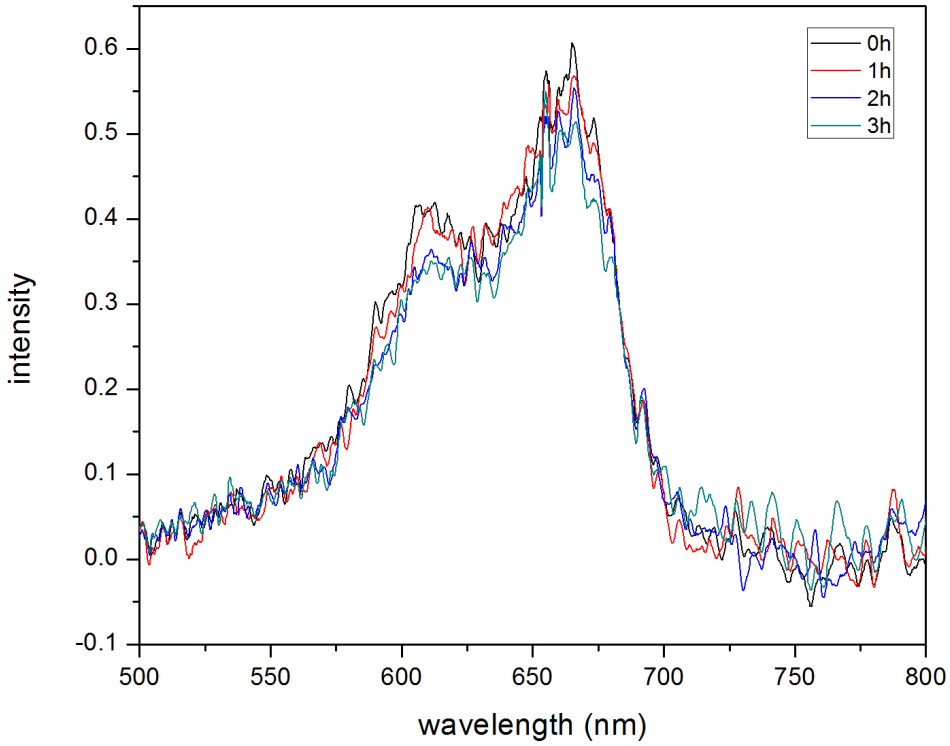

Figure 25: Graph of absorbance versus wavelength for 1.0g NaCl methylene blue solution

The figure 26 below shows the degradation of methylene blue solution with 1.5g NaCl under visible light. After 3 hours, the degradation of methylene blue dye is 13.7%.

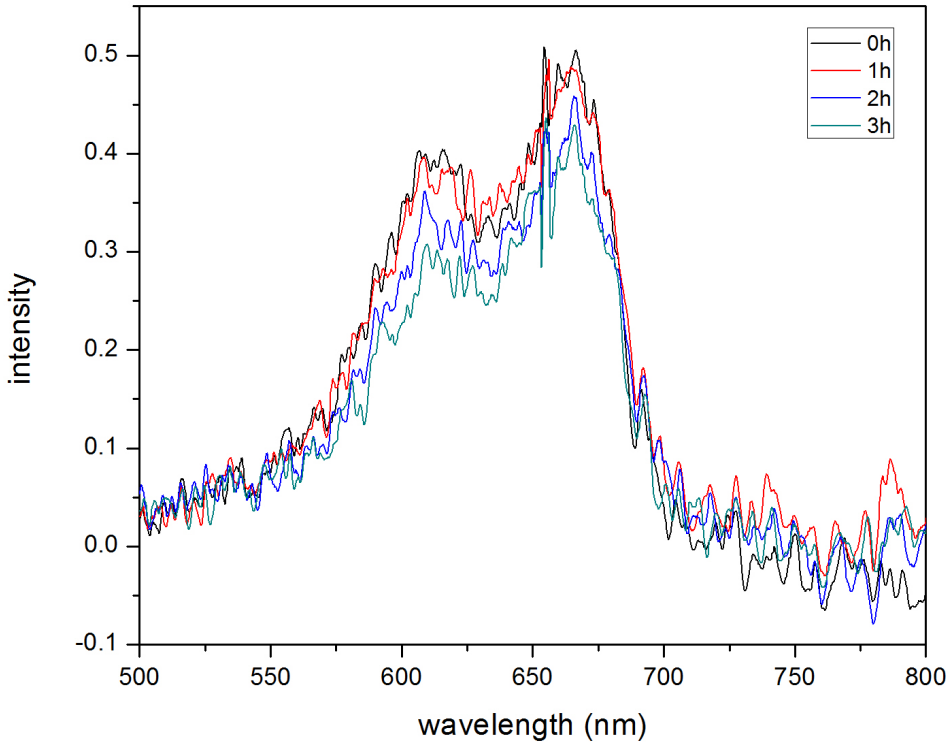

Figure 26: Graph of absorbance versus wavelength for 1.5g NaCl methylene blue solution

The table 5 below shows the degradation percentage for these four different salinity solutions at a time of 180 minutes.

Table 7: Degradation percentages of different salinity solutions under visible light at 180 minutes

	0g NaCl (pH=5)	10.5g NaCl (pH=6)	1.0g NaCl (pH=6.5)	1.5g NaCl (pH=7)
Irradiation Time(minutes)	180	180	180	180
Percentage Degradation	32.2%	18.2%	16.6%	13.7%

5.4.2 Comparative analysis of photolytic degradation under UV light

In order to better compare the degradation of methylene blue for these four different salinity solutions under visible light. The figure 27 below shows the absolute value of absorbance intensity C/C_o (Y-axis), which means the percentage of the absorbance value at time C to the one at time Co=0 minute, changing as the time (X-axis) increases up to 180 minutes.

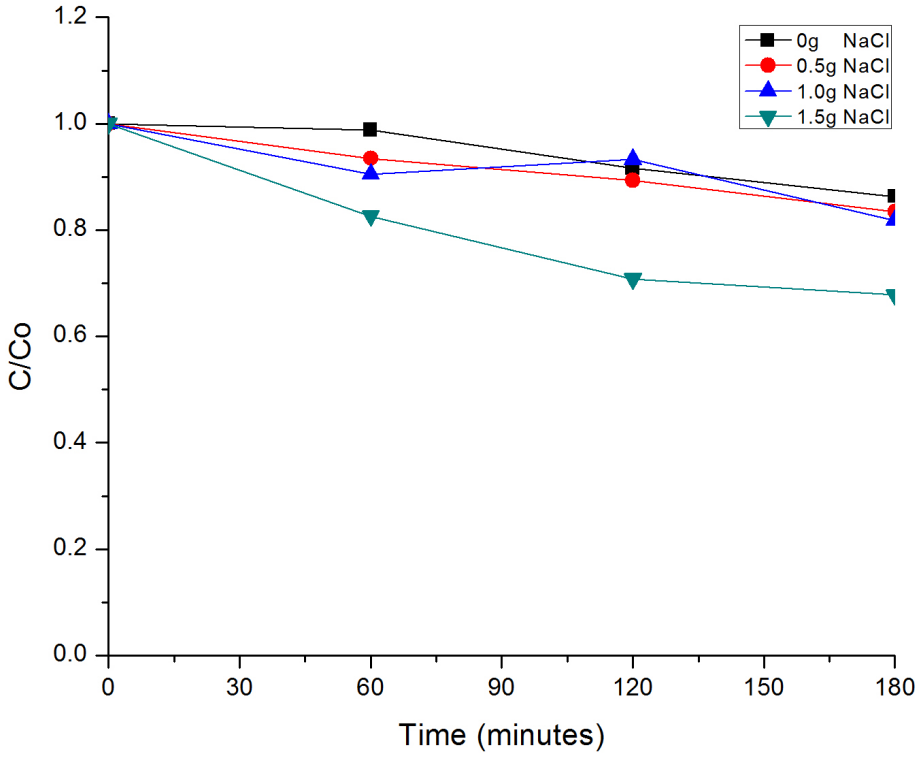

Figure 27: Graph of the degradation of four different salinity solutions under visible light

Therefore, it can tell from the figure 27 show above that NaCl has a negative influence for methylene blue photolysis under visible light. Less salinity might contribute to methylene blue solution photolysis.

Chapter 6: Conclusions

In this project, WO_3/PANI hybrid photocatalyst was synthesized, along with the TiO_2/PANI thin film based on the same method. The photocatalytic activities of WO_3/PANI, TiO_2/PANI thin film and pure WO_3 respectively were tested under visible light by monitoring the decomposition methylene blue solutions. The outcome of UV-Vis spectroscopy is that the degradation of methylene blue solution was the highest for the WO_3/PANI thin film photocatalyst, which displayed a 88.3% degradation when exposed to visible light, and in comparison, the degradation of methylene blue solution by TiO_2/PANI and pure WO_3 was 62.4% and 39.1% respectively. Furthermore, the WO_3/PANI thin film was characterized via SEM, EDS in order to obtain the morphology of the samples, and TGA was used to analyze the weight percentages of the various components in the sample.

The natural photolysis of methylene blue solution was also observed as a function of the salinity of the solution. 0g, 0.5g, 1.0g and 1.5g of NaCl particles were added into the methylene blue solution, and as deduced by the UV-Vis test, the one without NaCl show more efficient methylene photolysis, the degradation rate being 32.2%. The solutions containing 0.5g, 1.0g and 1.5g NaCl respectively had degradation rates of 18.2%, 16.6%, and 13.7% respectively.

Future work

Even though the WO_3/PANI hybrid photocatalyst showed good photocatalytic activities according to UV-vis spectroscopy test, there are still two main problems left in this work: (1) the conductivity of the sample is low; (2) the uniformity of the sample is limited. For the first problem, there are two ways we can try to improve the conductivity: one way is to make the WO_3 and PANI uniformly in a single layer instead of double layers, or the other way is to make a triple layers -- one PANI layer in the middle and two WO_3 layers on the both sides. For the second problem: a better way is to improve the coating methods to make the WO_3 particles dispersed even better and more evenly.

Reference

[1] Hofmann, Michael R., et al. "Environmental applications of semiconductor photocatalysis." Chem Rev 95.1 (1995): 69-96.

[2] Mills, Andrew, and Stephen Le Hunte. "An overview of semiconductor photocatalysis." Journal of photochemistry and photobiology A: Chemistry 108.1 (1997): 1-35.

[3] Fujishima, Akira, and Kenichi Honda. "Electrochemical photolysis of water at a semiconductor electrode." nature 238 (1972): 37-8.

[4] Frank, Steven N., and Allen J. Bard. "Heterogeneous photocatalytic oxidation of cyanide and sulfite in aqueous solutions at semiconductor powders." The Journal of Physical Chemistry 81.15 (1977): 1484-1488.

[5] Markham, Maria C., and Keith J. Laidler. "A Kinetic Study of Photo-oxidations on the Surface of Zinc Oxide in Aqueous Suspensions." The Journal of Physical Chemistry 57.3 (1953): 363-369.

[6] Jusang Lee. "Synthesis and Characterization of Nanostructured Metal Oxide for Water Remediation and Energy Applications." Doctoral Dissertation, Stony Brook University, December 2013.

[7] Maira, A_J, et al. "Gas-phase photo-oxidation of toluene using nanometer-size TiO_2 catalysts." Applied Catalysis B: Environmental 29.4 (2001): 327-336.

[8] Fox M A, Dulay M T. "Heterogeneous photocatalysis." Chem Rev, 1993, 93:341-357.

[9] Hagfeldt, Anders, and Michael Graetzel. "Light-induced redox reactions in nanocrystalline systems." Chemical Reviews 95.1 (1995): 49-68.

[10] Linsebigler, Amy L., Guangquan Lu, and John T. Yates Jr. "Photocatalysis on TiO_2 surfaces: principles, mechanisms, and selected results." Chemical reviews 95.3 (1995): 735-758.

[11] Peral, Jose, Xavier Domenech, and David F. Ollis. "Heterogeneous photocatalysis for purification, decontamination and deodorization of air." Journal of Chemical Technology and Biotechnology 70.2 (1997): 117-140.

[12] N Serpone, E Pellizzetti. "Photocatalysis: Fundamentals and Applications." Wiley, New York, 1989.

[13] Sayilkan, Funda, et al. "Hydrothermal Synthesis, Characterization and Photocatalytic Activity of Nanosized TiO_2 Based Catalysts for Rhodamine B Degradation." Turkish Journal of Chemistry 31.2 (2007): 211-221.

[14] Kang, E. T., K. G. Neoh, and K. L. Tan. "Polyaniline: a polymer with many interesting intrinsic redox states." Progress in Polymer Science 23.2 (1998): 277-324.

[15] Huang, Wu-Song, Brian D. Humphrey, and Alan G. MacDiarmid. "Polyaniline, a novel conducting polymer. Morphology and chemistry of its oxidation and reduction in aqueous electrolytes." Journal of the Chemical Society, Faraday Transactions 1: Physical Chemistry in Condensed Phases 82.8 (1986): 2385-2400.

[16] Inzelt, G., et al. "Electron and proton conducting polymers: recent developments and prospects." Electrochimica Acta 45.15 (2000): 2403-2421.

[17] Zhang, Hao, Ruilong Zong, and Yongfa Zhu. "Photocorrosion inhibition and photoactivity enhancement for zinc oxide via hybridization with monolayer polyaniline." The Journal of Physical Chemistry C 113.11 (2009): 4605-4611.

[18] Zhang, H.; Zhu, Y. J. Phys. Chem. C 2010, 5822−5826.

[19] Xu, Yong, and Martin AA Schoonen. "The absolute energy positions of conduction and valence bands of selected semiconducting minerals." American Mineralogist 85.3-4 (2000): 543-556.

[20] Fujishima, Akira, Tata N. Rao, and Donald A. Tryk. "TiO_2 photocatalysts and diamond electrodes." Electrochimica acta 45.28 (2000): 4683-4690.

[21] Colmenares, Juan Carlos, et al. "Nanostructured photocatalysts and their applications in the photocatalytic transformation of lignocellulosic biomass: an overview." Materials 2.4 (2009): 2228-2258.

[22] Childs, Ronald F., and Mark E. Hagar. "Photo-and thermal isomerization of some 1-methoxyallyl cations." Canadian Journal of Chemistry 58.17 (1980): 1788-1794.

[23] Pelizzetti, Ezio, et al. "Photocatalytic degradation of nonylphenol ethoxylated surfactants." Environmental science & technology 23.11 (1989): 1380-1385.

[24] Tang, W. Z., et al. "TiO_2/UV photodegradation of azo dyes in aqueous solutions." Environmental technology 18.1 (1997): 1-12.

[25] Sauer, T., et al. "Kinetics of photocatalytic degradation of reactive dyes in a TiO_2 slurry reactor." Journal of Photochemistry and Photobiology A: Chemistry 149.1 (2002): 147-154.

[26] Dvoranova, Dana, et al. "Investigations of metal-doped titanium dioxide photocatalysts." Applied Catalysis B: Environmental 37.2 (2002): 91-105.

[27] Gaya, Umar Ibrahim, and Abdul Halim Abdullah. "Heterogeneous photocatalytic degradation of organic contaminants over titanium dioxide: a review of fundamentals, progress and problems." Journal of Photochemistry and Photobiology C: Photochemistry Reviews 9.1

(2008): 1-12.

[28] Glaze, William H., Joon-Wun Kang, and Douglas H. Chapin. "The chemistry of water treatment processes involving ozone, hydrogen peroxide and ultraviolet radiation." (1987): 335-352.

[29] Sakthivel, S., et al. "Solar photocatalytic degradation of azo dye: comparison of photocatalytic efficiency of ZnO and TiO_2." Solar Energy Materials and Solar Cells 77.1 (2003): 65-82.

[30] Matsuda, Satoru, Hiroyuki Hatano, and Atsushi Tsutsumi. "Ultrafine particle fluidization and its application to photocatalytic NO_x treatment." Chemical Engineering Journal 82.1 (2001): 183-188.

[31] Paririe, M. R. "An Investigation of TiO_2 photocatalysis for the treatment of water contaminated with metals and organic chemical." Environment Science and Technology 27.9 (1993): 1776-1782.

[32] Muszkat, Lea, et al. "Photocatalytic degradation of pesticides and biomolecules in water." Pest management science 58.11 (2002): 1143-1148.

[33] Kogo, Katsuyuki, Hiroshi Yoneyama, and Hideo Tamura. "Photocatalytic oxidation of cyanide on platinized titanium dioxide." The Journal of Physical Chemistry 84.13 (1980): 1705-1710.

[34] Ding, Hanming, Hong Sun, and Yongkui Shan. "Preparation and characterization of mesoporous SBA-15 supported dye-sensitized TiO_2 photocatalyst." Journal of Photochemistry and Photobiology A: Chemistry 169.1 (2005): 101-107.

[35] Diebold, Ulrike. "The surface science of titanium dioxide." Surface science reports 48.5 (2003): 53-229.

[36] Mohammadi, M. R., et al. "Preparation of high surface area titania (TiO_2) films and powders using particulate sol–gel route aided by polymeric fugitive agents." Sensors and Actuators B: Chemical 120.1 (2006): 86-95.

[37] Maira, A_J, et al. "Gas-phase photo-oxidation of toluene using nanometer-size TiO_2 catalysts." Applied Catalysis B: Environmental 29.4 (2001): 327-336.

[38] Liao, D. L., C. A. Badour, and B. Q. Liao. "Preparation of nanosized TiO_2/ZnO composite catalyst and its photocatalytic activity for degradation of methyl orange." Journal of Photochemistry and Photobiology A: Chemistry 194.1 (2008): 11-19.

[39] Krýsa, Josef, et al. "The effect of thermal treatment on the properties of TiO_2 photocatalyst." Materials Chemistry and Physics 86.2 (2004): 333-339.

[40] Chun, Hu, Wang Yizhong, and Tang Hongxiao. "Destruction of phenol aqueous solution by photocatalysis or direct photolysis." Chemosphere 41.8 (2000): 1205-1209.

[41] Saquib, M., and M. Muneer. "TiO_2-mediated photocatalytic degradation of a triphenylmethane dye (gentian violet), in aqueous suspensions." Dyes and Pigments 56.1 (2003): 37-49.

[42] Arana, J., et al. "Photocatalytic degradation of formaldehyde containing wastewater from veterinarian laboratories." Chemosphere 55.6 (2004): 893-904.

[43] Curcó, D., et al. "Effects of radiation absorption and catalyst concentration on the photocatalytic degradation of pollutants." Catalysis Today 76.2 (2002): 177-188.

[44] Ustinovich, Elena A., Dmitry G. Shchukin, and Dmitry V. Sviridov. "Heterogeneous photocatalysis in titania-stabilized perfluorocarbon-in-water emulsions: Urea photosynthesis and chloroform photodegradation." Journal of Photochemistry and Photobiology A: Chemistry 175.2 (2005): 249-252.

[45] Qamar, M., M. Muneer, and D. Bahnemann. "Heterogeneous photocatalysed degradation of two selected pesticide derivatives, triclopyr and daminozid in aqueous suspensions of titanium dioxide." Journal of Environmental Management 80.2 (2006): 99-106.

[46] Shourong, Zheng, et al. "A study on dye photoremoval in TiO_2 suspension solution." Journal of Photochemistry and Photobiology A: Chemistry 108.2 (1997): 235-238.

[47] Haque, M. M., and M. Muneer. "Photodegradation of norfloxacin in aqueous suspensions of titanium dioxide." Journal of Hazardous Materials 145.1 (2007): 51-57.

[48] Mansilla, H. D., et al. "Photocatalytic EDTA degradation on suspended and immobilized TiO_2." Journal of Photochemistry and Photobiology A: Chemistry 181.2 (2006): 188-194.

[49] S. Divya. "electrospun nanocomposites for degradation of dyes in water using metal oxide photocatalysts." Master thesis, August 2013.

[50] S. Sood. "polymorphism control in nanostructured metal oxides." Doctoral Dissertation, August 2014.

[51] Lassner, Erik, and Wolf-Dieter Schubert. Tungsten: properties, chemistry, technology of the elements, alloys, and chemical compounds. Springer Science & Business Media, 1999.

[52] Loopstra, B. O., and H. M. Rietveld. "Further refinement of the structure of WO_3." Acta Crystallographica Section B: Structural Crystallography and Crystal Chemistry 25.7 (1969): 1420-1421.

[53] Deb, Satyen K. "Opportunities and challenges in science and technology of WO_3 for electrochromic and related applications." Solar Energy Materials and Solar Cells 92.2 (2008):

245-258.

[54] Zheng, Haidong, et al. "Nanostructured tungsten oxide–properties, synthesis, and applications." Advanced Functional Materials 21.12 (2011): 2175-2196.

[55] Monllor Satoca, Damián, et al. "Photoelectrochemical Behavior of Nanostructured WO_3 Thin Film Electrodes: The Oxidation of Formic Acid." ChemPhysChem 7.12 (2006): 2540-2551.

[56] Baeck, S H., et al. "Enhancement of photocatalytic and electrochromic properties of electrochemically fabricated mesoporous WO_3 thin films." Advanced Materials 15.15 (2003): 1269-1273.

[57] Cui, Xiangzhi, et al. "Platinum/mesoporous WO_3 as a carbon-free electrocatalyst with enhanced electrochemical activity for methanol oxidation." The Journal of Physical Chemistry B 112.38 (2008): 12024-12031.

[58] Akiyama, Morito, et al. "Tungsten Oxide-Based Semiconductor Sensor Highly Sensitive to NO and NO_2." Chemistry Letters 9 (1991): 1611-1614.

[59] Sun, Hong-Tao, et al. "Microstructural effect on NO_2 sensitivity of WO_3 thin film gas sensors Part 1. Thin film devices, sensors and actuators." Thin Solid Films 287.1 (1996): 258-265.

[60] Granqvist, Claes G. "Electrochromic tungsten oxide films: review of progress 1993–1998." Solar Energy Materials and Solar Cells 60.3 (2000): 201-262.

[61] Zhang, J., et al. "Enhanced electrochromic performance of macroporous WO_3 films formed by anodic oxidation of DC-sputtered tungsten layers." Electrochimica Acta 55.23 (2010): 6953-6958.

[62] Cheng, Wei, et al. "Synthesis and electrochromic properties of mesoporous tungsten oxideBasis of a presentation given at Materials Discussion No. 3, 26–29 September, 2000, University of Cambridge, UK." Journal of Materials chemistry 11.1 (2001): 92-97.

[63] H. Shirakawa, E.J. Louis, A.C. MacDiarmid, C.K. Chiang, A.J Heeger. J.Chem.Soc.Commun. 1977, p. 578.

[64] Gerard, Manju, Asha Chaubey, and B. D. Malhotra. "Application of conducting polymers to biosensors." Biosensors and Bioelectronics 17.5 (2002): 345-359.

[65] Rudge, Andy, et al. "A study of the electrochemical properties of conducting polymers for application in electrochemical capacitors." Electrochimica Acta 39.2 (1994): 273-287.

[66] Jing Zhang. "Polyaniline and Cellulose Acetate Chemomechanical Actuator and its Selectivity for Acetone. " Master Thesis, Stony Brook University, May 2014.

[67] E.T. Kang, K.G. Neoh, K.L. Tan, Prog. Polym. Sci. 23(1988) p 227-324.

[68] S.M. Hassan, A.G. Baker, H. I. Jafaar. International Journal of Basic and Applied Science, vol 01, No. 02, Oct 2012, p 352-362.

[69] Li, Dan, Jiaxing Huang, and Richard B. Kaner. "Polyaniline nanofibers: a unique polymer nanostructure for versatile applications." Accounts of chemical research 42.1 (2008): 135-145.

[70] MacDiarmid, A. G., et al. "Polyaniline: a new concept in conducting polymers." Synthetic Metals 18.1 (1987): 285-290.

[71] Carlin C.M., Kapley L.J., Bard A.J., J. Electronchem. Soc.1985. (132), 353.

[72] Genies, E. M., et al. "Polyaniline: a historical survey." Synthetic Metals 36.2 (1990): 139-182.

[73] Wang F., Tang J., Jing X., Ni S., Wang B., Applied Chemistry, 1990, (5), 4.

[74] Zhang G., Bi X., ACTA POLYMERICA SINICA, 1994 (1), 55-59.

[75] Sinha, R. Outlines of Polymer Technology: Manufacture of Polymers. PHI Learning Pvt. Ltd., 2004.

[76] V.R. Gowariker, N.V. Viswanathan, J. Sreedhar, Polymer Science, New Delhi, 1999.

[77] Pron, A., et al. "Flexible, highly transparent, and conductive polyaniline cellulose acetate composite films." Journal of applied polymer science 63.8 (1997): 971-977.

[78] H. K. Lonsdale, U. Merten andR. L. Riley. J. Applied Polymer Science Volume 9, Issue 4, p1341–1362, April 1965.

[79] Lei Liu, Zhigang Shen, Shuaishuai Liang, Min Yi, Xiaojing Zhang, Shulin Ma J. Appl. Polym. Sci. 2014, DOI: 10.1002/p40292.

[80] Xiangling Ren, Dong Chen, Xianwei Meng, Fangqiong Tang, Aiming Du, Lin Zhang. Biointerfaces Volume 72, Issue 2, 1 September 2009, P188–192.

[81] Norrman, K., A. Ghanbari-Siahkali, and N. B. Larsen. "6 Studies of spin-coated polymer films." Annual Reports Section" C"(Physical Chemistry) 101 (2005): 174-201.

[82] El Qada, Emad N., Stephen J. Allen, and Gavin M. Walker. "Adsorption of methylene blue onto activated carbon produced from steam activated bituminous coal: a study of equilibrium adsorption isotherm." Chemical engineering journal 124.1 (2006): 103-110.

[83] Chandrasekhar, Sathy, and P. N. Pramada. "Rice husk ash as an adsorbent for methylene blue—effect of ashing temperature." Adsorption 12.1 (2006): 27-43.

[84] Jian-xiao, L. V., et al. "Decoloration of methylene blue simulated wastewater using a UV-H_2O_2 combined system." Journal of Water Reuse and Desalination 1.1 (2011): 45-51.

[85] Gillman, P. K. "Methylene blue implicated in potentially fatal serotonin toxicity." Anaesthesia 61.10 (2006): 1013-1014.

[86] Gillman, P. Ken, et al. "Methylene blue is a potent monoamine oxidase inhibitor." Canadian Journal of Anesthesia/Journal canadien d'anesthésie 55.5 (2008): 311-312.

[87] Salah, Manal, Nevien Samy, and Maha Fadel. "Methylene blue mediated photodynamic therapy for resistant plaque psoriasis." Journal of drugs in dermatology: JDD 8.1 (2009): 42-49.

[88] Schirmer, R. Heiner, et al. "Methylene blue as an antimalarial agent." Redox Report 8.5 (2003): 272-275.

[89] Meissner, Peter E., et al. "Methylene blue for malaria in Africa: results from a dose-finding study in combination with chloroquine." Malaria journal 5.1 (2006): 84.

[90] Zendehdel, M., et al. "Removal of methylene blue dye from wastewater by adsorption onto semi-inpenetrating polymer network hydrogels composed of acrylamide and acrylic acid copolymer and polyvinyl alcohol." Iranian Journal of Environmental Health Science & Engineering 7.5 (2010): 431-436.

[91] Houas, Ammar, et al. "Photocatalytic degradation pathway of methylene blue in water." Applied Catalysis B: Environmental 31.2 (2001): 145-157.

[92] Tang, Junwang, et al. "Photocatalytic degradation of methylene blue on $CaIn_2O_4$ under visible light irradiation." Chemical physics letters 382.1 (2003): 175-179.

[93] Kwon, Chul Han, et al. "Degradation of methylene blue via photocatalysis of titanium dioxide." Materials Chemistry and Physics 86.1 (2004): 78-82.

[94] Lin, Yaw-Jian, et al. "Enhanced photocatalysis of pentachlorophenol by metal-modified titanium (IV) oxide." Journal of Environmental Science and Health Part B: Pesticides, Food Contaminants, and Agricultural Wastes 41.7 (2006): 1143-1158.

[95] Salem, Ibrahim A., and Mohamed S. El-Maazawi. "Kinetics and mechanism of color removal of methylene blue with hydrogen peroxide catalyzed by some supported alumina surfaces." Chemosphere 41.8 (2000): 1173-1180.

[96] Eilers, J. M., T. J. Sullivan, and K. C. Hurley. "The most dilute lake in the world?" Hydrobiologia 199.1 (1990): 1-6.

[97] Anati, David A. "The salinity of hypersaline brines: concepts and misconceptions." International Journal of Salt Lake Research 8.1 (1999): 55-70.

[98] Gillet, Marcel, Romain Delamare, and Eveline Gillet. "Growth of epitaxial tungsten oxide nanorods." Journal of Crystal Growth 279.1 (2005): 93-99.